2022년 2월
석사학위논문

Odontoclastogenesis induced by 25-hydroxycholesterol in MDPC-23 mouse odontoblast-like cell line

조선대학교 대학원

치의생명공학과

임 향 이

Odontoclastogenesis induced by 25-hydroxycholesterol in MDPC-23 mouse odontoblast-like cell line

MDPC-23 상아질모세포에서
25-hydroxycholesterol에 의한 파치세포화

2022년 2월 25일

조선대학교 대학원

치의생명공학과

임 향 이

Odontoclastogenesis induced by 25-hydroxycholesterol in MDPC-23 mouse odontoblast-like cell line

지도교수 김 재 성

이 논문을 이학 석사학위신청 논문으로 제출함.

2021년 10월

조선대학교 대학원

치의생명공학과

임 향 이

임향이의 석사학위논문을 인준함

위원장 조선대학교 교 수 김 흥 중 (인)

위 원 조선대학교 교 수 김 도 경 (인)

위 원 조선대학교 교 수 김 재 성 (인)

2021년 12월

조선대학교 대학원

TABLE OF CONTENT

LIST OF TABLES ····· iii
LIST OF FIGURES ····· iv
LIST OF ABBREVIATIONS ····· vi
ABSTRACT ····· viii

Ⅰ. INTRODUCTION ····· 1

Ⅱ. MATERIALS AND METHODS ····· 4

Ⅱ- 1. Chemicals ····· 4
Ⅱ- 2. Cell line and cell culture ····· 4
Ⅱ- 3. Cell counting kit-8 (CCK-8) ····· 4
Ⅱ- 4. Cell survival assay ····· 5
Ⅱ- 5. TRAP staining and activity assay ····· 5
Ⅱ- 6. Hematoxylin & eosin (H&E) staining ····· 6
Ⅱ- 7. Reactive oxygen species (ROS) detection ····· 6
Ⅱ- 8. Western blotting ····· 6
Ⅱ- 9. Quantitative polymerase chain reaction (qPCR) ····· 7
Ⅱ-10. Immunocytochemistry ····· 7
Ⅱ-11. Gelatin zymography ····· 8
Ⅱ-12. Dentine resorption assay ····· 8
Ⅱ-13. Measurement of prostaglandin E_2 (PGE_2) Production ····· 9
Ⅱ-14. Statistical analysis ····· 9

Ⅲ. RESULTS ····· 10

Ⅲ- 1. CH25H upregulates the synthesis of 25-HC in lipopolysaccharide (LPS)-treated MDPC-23 cells ····· 10

Ⅲ- 2. 25-HC does not affect the viability of MDPC-23 cells ····· 10
Ⅲ- 3. 25-HC induces the odontoclastogenesis of MDPC-23 cells ····· 11
Ⅲ- 4. 25-HC accelerates dentin resorption in MDPC-23 cells through the upregulation of MMP-2 and MMP-9 ····· 12
Ⅲ- 5. 25-HC promotes odontoclastogenesis through the nuclear translocation of NF-κB-NFATc1 from the cytosol in MDPC-23 cells ····· 13
Ⅲ- 6. 25-HC induces odontoclastogenesis in MDPC-23 cells by upregulating RANKL ····· 13
Ⅲ- 7. 25-HC induces the production of ROS in MDPC-23 cells through the Rac1/2/3-nicotinamide adenine dinucleotide phosphate oxidase 1(NOXO1) axis ····· 14
Ⅲ- 8. 25-HC upregulates the expression of inflammatory mediators and pro-inflammatory cytokines in MDPC-23 cells through the modulation of the nuclear factor erythroid-2-related factor 2 (Nrf2)-heme oxygenase-1 (HO-1) axis ····· 15
Ⅲ- 9. 25-HC induces odontoclastogenesis in MDPC-23 cells through the activation of the NF-κB cellular signaling pathway ····· 16

Ⅳ. DISCUSSION ····· 18

Ⅴ. REFERENCES ····· 24

TABLES ····· 32

FIGURES ····· 34

국문초록 ····· 48

감사의 글 ····· 50

LIST OF TABLES

Table 1. Western blot antibody conditions used in this study ····· 32

Table 2. PCR primer sequences used in this study ····· 33

LIST OF FIGURES

Figure 1. The chemical structure of 25-HC ····· 34

Figure 2. LPS upregulates the levels of CH25H and 25-HC in MDPC-23 cells ····· 35

Figure 3. 25-HC does not affect the viability of MDPC-23 cells ····· 36

Figure 4. 25-HC increases the number of odontoclasts differentiated from MDPC-23 cells ····· 37

Figure 5. 25-HC promotes dentin resorption in the odontoclasts differentiated from MDPC-23 cells ····· 38

Figure 6. 25-HC promotes dentin resorption in odontoclasts differentiated from MDPC-23 cells through the upregulation and activation of MMPs ····· 39

Figure 7. 25-HC promotes the expression of odontoclastogenic biomarkers and the nuclear translocation of NF-κB in MDPC-23 cells ····· 40

Figure 8. 25-HC promotes odontoclastogenesis in MDPC-23 cells through the upregulation of RANKL and RANK and the downregulation of OPG ····· 41

Figure 9. 25-HC promotes ROS production in MDPC-23 cells through the Rac1/2/3-NOXO1 axis ····· 42

Figure 10. 25-HC upregulates the expression of inflammatory mediators and pro-inflammatory cytokines in MDPC-23 cells through the modulation of Nrf2-HO-1 axis ····· 43

Figure 11. NF-κB inhibitor suppresses odontoclastogenesis in 25-HC-treated MDPC-23 cells ····· 44

Figure 12. NF-κB inhibitor suppresses the expression of odontoclastogenic factors in 25-HC-treated MDPC-23 cells ····· 45

Figure 13. 25-HC induces odontoclastogenesis through the modulation of the NF-κB signaling pathway in MDPC-23 cells ····· 46

Figure 14. The schematic diagram of 25-HC-induced odontoclastogenesis in the MDPC-23 cells ····· 47

LIST OF ABBREVIATIONS

25-HC ····· 25-hydroxycholesterol
BSA ····· Bovine serum albumin
CCK-8 ····· Cell counting kit-8
CDDO-Me ····· Bardoxolone methyl; CDDO-methyl ester
CH25H ····· Cholesterol 25-hydroxylase
COX-2 ····· Cyclooxygenase-2
DAPI ····· 4’,6-Diamidino-2-phenylindole dihydrochloride
DMEM ····· Dulbecco’s modified eagls’s medium
DMSO ····· Dimethyl sulfoxide
DPBS ····· Dulbecco's phosphate-buffered saline
ELISA ····· Enzyme-linked immunosorbent assay
FBS ····· Fetal bovine serum
GAPDH ····· Glyceraldehyde 3-phosphate dehydrogenase
H&E ····· Hematoxylin & eosin
H2DCF-DA ····· 2′,7′-dichlorfluorescein-diacetate
HO-1 ····· Heme oxygenase-1
iNOS ····· Inducible nitric oxide synthase
IL-6 ····· Interleukin-6
LPS ····· Lipopolysaccharides
M-CSF ····· Macrophage colony stimulating factor
MMPs ····· Matrix metalloproteinases
NADPH ····· Nicotinamide-adenine dinucleotide phosphate
NFATc1 ····· Nuclear factor of activated T cells, cytoplasmic 1
NF-κB ····· Nuclear factor-κB
NOXO1 ····· Nicotinamide-adenine dinucleotide phosphate oxidase organizer 1
Nrf2 ····· Nuclear factor erythroid 2-related factor 2
OPG ····· Osteoprotegerin

PBS ····· Phosphate buffered saline
PGE_2 ····· Prostaglandin E_2
PVDF ····· Polyvinylidene fluoride
qPCR ····· quantitative polymerase chain reaction
RANK ····· Receptor activator of nuclear factor-κB
RANKL ····· Receptor activator of nuclear factor-κB ligand
ROS ····· Reactive oxygen species
SDS-PAGE ····· Sodium dodecyl Sulfate polyacrylamide gel electrophoresis
TBS-T ····· Tris buffered saline with tween 20
TNF-α ····· Tumor necrosis factor-α
TRAF6 ····· Tumor necrosis factor receptor associated factor 6
TRAP ····· Tartrate-resistant acid phosphate

ABSTRACT

Odontoclastogenesis induced by 25-hydroxycholesterol in MDPC-23 mouse odontoblast-like cell line

Lim, HyangI
Advisor : Prof. Kim, Jae-Sung, Ph.D.
Department of Biodental Engineering
Graduate school of Chosun University

Aim: To investigate the ability of 25-hydroxycholesterol (25-HC) to induce odontoclastogenesis in MDPC-23 odontoblast-like cells and the underlying mechanisms.

Methodology: 25-HC-induced odontocalst differentiation was investigated by tartrate-resistant acid phosphate (TRAP) staining and activity assay, western blotting using specific antibodies, immunocytochemistry, and dentin resorption assay. Furthermore, to investigate the effects of ROS production in 25-HC by MDPC-23 cells.

Results: Lipopolysaccharide (LPS) promoted inflammation, odontoclast differentiation, and cholesterol-25-hydroxylase (CH25H) expression in MDPC-23 cells. This indicated that LPS induces odontoclastogenesis by promoting the synthesis of 25-HC through the upregulation of CH25H. Treatment with 25-HC upregulated TRAP activity and increased the number of multinucleated cells in MDPC-23 cells (a morphological characteristic of odontoclast). Additionally, 25-HC upregulated the expression and activity of resorption enzymes, such as matrix metalloproteinase (MMP)-9 and MMP-2 in odontoclast differentiated from MDPC-23 cells. Furthermore, 25-HC upregulated the production of reactive oxygen species in MDPC-23 cells through the Rac1/2/3-NOXO1 axis. In addition to upregulating inflammatory mediators, such as iNOS, COX-2 and PGE_2, 25-HC upregulated pro-inflammatory cytokines, such as TNF-α and IL-6 in MDPC-23

cells through the nuclear factor erythroid 2-related factor 2 (Nrf2)-heme oxygenase-1 (HO-1) axis. RANKL-RANK mediated the 25-HC-induced odontoclast differentiation of MDPC-23 cells. Odontoclast differentiation markers, such as TRAF6, NFATc1, cathepsin K, nuclear factor-κB (NF-κB) and c-fos, were upregulated in 25-HC-treated MDPC-23 cells. Furthermore, 25-HC promoted the nuclear translocation of NF-κB from the cytosol in MDPC-23 cells. Treatment with the NF-κB inhibitor downregulated TRAP activity and the expression of odontoclastogenesis factor in 25-HC-treated MDPC-23 cells.

Conclusions: Thus, 25-HC induced odontoclast differentiation through the odontoclastogenesis factor-mediated activation of NF-κB and upregulated inflammatory mediators through the modulation of the nuclear factor Nrf2-HO-1 axis in MDPC-23 cells.

I. INTRODUCTION

Teeth, which are the hardest of human tissues with an important role in speech and chewing, comprise various hard substances and tissues, such as enamel, dentin, cementum, and periodontal ligaments [1]. In particular, the thick dentin layer of tooth is a major components of mineralized dental tissues [2]. Dentin, which comprises microscopic tubules, is covered by a crown that is composed of highly mineralized enamel [3]. Upon loss of the enamel, various stimuli, such as heat or cold are transduced to the underlying nerves through the microscopic tubules, which leads to sensitivity or pain [4]. Therefore, the maintenance of dentin is critical for the optimal functioning of teeth [4]. Odontoblasts synthesize dentin through a process called dentinogenesis [4].

In a mature tooth, odontoblasts are arranged along the interface between the dental pulp and dentin from the crown to the cervix and the root apex [2]. In addition, to regulating the formation of physiological primary and secondary dentins through the synthesis of an organic matrix mainly comprising type I collagen, odontoblasts modulate the mineralization of dentins through the secretion of proteoglycans and non-collagenous proteins that are involved in the nucleation and the regulation of cell growth during the mineral phase [2]. Recent studies have reported that odontoblasts, which function as sensor cells, are susceptible to bacterial invasion in dental caries [5-6]. Bacterial invasion leads to the elicitation of the pulp immune and inflammatory responses [6]. Odontoblasts are reported to possess ion channels and are closely associated with mechanotransduction or nociception, which mediates tooth pain sensation response to sense external stimuli [7]. Hence, the maintenance of odontoblasts and dentin is critical for the preservation of tooth function through the regulation of fundamental dentinogenic activities and tooth pain.

The resorption of dentin is mediated by odontoclasts, which are multinucleated giant cells with morphological structures and biological functions similar to those of osteoclasts associated with the absorption of bone tissue [8]. Odontoclasts and osteoclasts, characterized by abundant mitochondria and large vacuoles in their

cytoplasm, can absorb specific mineralized hard tissues through the production of resorption lacunae by secreting hydrogen ions and matrix-degrading enzymes [9]. Compared with osteoclasts, odontoclasts exhibit smaller size, fewer nuclei, smaller resorption lacunae, and are localized to hard tooth tissues [10]. The specific mechanisms underlying cellular differentiation and dental resorption of odontoclasts have not been elucidated. Odontoclasts differentiate from tartrate-resistant acid phosphatase (TRAP)-positive mononuclear cells [11]. Dental pulps with some cytokine-producing cells mediate the differentiation of odontoclast from the monocyte-macrophage lineage through the receptor activator of nuclear factor-κB ligand (RANKL)-receptor activator of nuclear factor-κB (RANK) system, which leads to the activation of nuclear transcription factors, including nuclear factor-κB (NF-κB) and nuclear factor of activated T-cells, cytoplasmic 1 (NFATc1) [11]. Next, precursor cells, such as monocytes or macrophages, differentiate into multinucleated cells with resorption activity [11].

The MDPC-23 cells established from the fetal mouse mandibular first molar papilla cells are considered to be odontoblast lineage cells with strong proliferative, odontoblast differentiative, and mineralization into dentin abilities [12]. Additionally, RANKL and macrophage colony stimulating factor (M-CSF) have been reported to induce odontoclastogenesis of odontoblast-like MDPC-23 cells [13]. Therefore, the odontoblast-like MDPC-23 cells are appropriate *in vitro* cell models to investigate the cellular mechanisms associated with odontoclastogenesis in dental pulp or papilla cells.

The oxidoreductase cholesterol-25-hydroxylase (CH25H), which catalyzes the synthesis of 25-hydroxycholesterol (25-HC, Figure 1), an oxysterol, from cholesterol, is upregulated in peripheral macrophages and dendritic cells under inflammatory conditions [14-15]. Recent studies have reported that 25-HC is involved in multiple physiological functions, such as innate and adaptive immunity, regulation of inflammation, protection against viral infection, formation of macrophage foam cells, production of immunoglobulin IgA, and cytokine production [16-19]. However, the physiological function of 25-HC in various cell types has not been characterized. Recently, Zhang et al. reported that 25-HC promotes RANKL-induced osteoclastogenesis in coordination with the NFATc1 and Sp1 complex in mouse bone marrow macrophages [20].

This study hypothesized that 25-HC is an inflammation-induced cholesterol metabolite that induces odontoclastogenesis in odontoblasts. Thus, this study aimed to investigate 25-HC-induced odontoclastogenesis and the underlying cellular mechanisms in odontoblast-like MDPC-23 cells.

Ⅱ. MATERIALS AND METHODS

Ⅱ-1. Chemicals

25-HC was purchased from Sigma-Aldrich (St. Louis, MO, USA) and was dissolved in ethyl alcohol at stock concentration 10 mg/mL. RANKL was purchased from PeproTech (Cranbury, NJ, USA) and was dissolved in phosphate-buffered saline (PBS, Welgene, Republic of Korea) add to 0.1% carrier protein (bovine serum albumin, BSA; Bioshop, Republic of Korea) at stock concentration 10 μg/mL. Bardoxolone methyl (CDDO-methyl ester; CDDO-Me) was purchased from Sigma-Aldrich and was dissolved in dimethyl sulfoxide (DMSO; Sigma-Aldrich) at stock concentration 50 mM.

Ⅱ-2. Cell line and cell culture

MDPC-23 cells, a mouse dental papilla cell, were grown in dulbecco modified eagle medium (DMEM; Welgene) containing 10% fetal bovine serum (FBS; Welgene) and antibiotics (50 unit/mL penicillin and 50 μg/mL streptomycin; Welgene) at 37℃ in a 5% CO_2-humidified atmosphere.

Ⅱ-3. Cell counting kit-8 (CCK-8)

MDPC-23 cells (1×10^3 cells/well) were grown in 48-well plates, and then treated with 25-HC. After 2, 4 and 6 days, the CCK-8 solution (Dojindo Molecular Technologies, Rockville, MD, USA) in dark condition. The plate were further cultured for 2 h. After incubation, the absorbance was read at 450 nm using a spectrometer (Epoch microplate spectrophotometer; BioTek, Winooski, VT, USA).

Ⅱ-4. Cell survival assay

Cell survival assay was performed to assess the survival of MDPC-23 treated with 25-HC using a Live and Dead assay kit (Molecular Probes, Eugene, OR, USA), which consists of green fluorescent calcein AM for labeling live cells and red flourescent ethidium homodimer-1 for labeling dead cells. MDPC-23 cells were cultured on 8-well chamber slides (Nunc Lab-Tek II Chamber Slide system; Sigma-Aldrich), and then treated with 25-HC for 2, 4, and 6 days. After incubation, cell survival assay was performed according to the manufacturer's instructions. Thereafter, the stained cells were imaged using a fluorescence microscope (Eclipse TE200; Nikon Instruments, Melville, NY, USA).

Ⅱ-5. TRAP staining and activity assay

Odontoclast differentiation effect of 25-HC on cells was measured by TRAP assay. MDPC-23 cells were cultured at a density of 1×10^3 cells/well in 8-well chamber slide and then treated with 50, 100, and 200 nM of 25-HC or 50 ng/mL RANKL for 6 days. After incubation, TRAP staining was performed. Briefly, the cells were rinsed with PBS and fixed with fixation solution [acetone, ethanol and citrate buffer (pH 5.4)]. After fixation, the cells were incubated with 0.5 M sodium tartrate buffer (pH 5.2) with fast red violet LB salt and naphthol-AS-BI-phosphate for TRAP activity (TaKaRa Bio Inc., Kyoto, Japan). TRAP-positive cells with three or more nuclei were considered as mature odontoclast. The cells were observed and imaged by Leica DM750 microscope (Leica Microsystems, Heerbrugg, Switzerland). Furthermore, TRAP activity assay was performed according to the manufacturer's instructions. Briefly, the cells were washed PBS and lysis with extraction solution. After lysis, the cells were incubated in ACP buffer (0.5 M sodium acetate, pH 5.2) with 10% sodium tartrate solution at 37℃ for 15 min. The TRAP activity was assessed by spectrophotometer at 405 nm.

Ⅱ-6. Hematoxylin & eosin (H&E) staining

H&E staining was performed to evaluate the morphological alterations of cells. MDPC-23 cells were cultured in 8-well chamber slide and treated with 50, 100, and 200 nM 25-HC or 50 ng/mL RANKL for 6 days. Subsequently, MDPC-23 cells were fixed with 4% paraformaldehyde for 15 min. After fixation, the cells were stained with hematoxylin (Abcam, Cambridge, UK) for 10 min and then differentiated with 1% hydrochloric acid ethanol for 1 min. Finally, the cells were stained with eosin (Abcam) for 1 min. The cells were observed and imaged using Leica DM750 microscope.

Ⅱ-7. Reactive oxygen species (ROS) detection

MDPC-23 cells were cultured at a density of 2×10^3 cells/well on 48 well plate with 50, 100, and 200 nM 25-HC or 50 ng/mL RANKL for 3 days. Three days later, the cell were washed with PBS, and detected using 2′,7′-dichlorfluorescein-diacetate (H2DCF-DA; Sigma-Aldrich) for 30 min at 37℃ in dark condition. Fluorescence was measured using a fluorescent microplate reader (Thermo Fisher Scientific, Waltham, MA, USA) and fluorescence microscope. Fluorescent microplate reader was measured at an excitation wavelength of 485 nm and an emission wavelength of 520 nm.

Ⅱ-8. Western blotting

MDPC-23 cells were seeded in a 6-well plate (1×10^5 cells/well) and treated with 25-HC for 6 days. Thereafter, MDPC-23 cells were lysed in ice-cold cell lysis buffer (Cell Signaling Technology, Danvers, MA, USA) containing phosphatase inhibitor cocktail (MedchemExpress, Monmouth junction, NJ, USA), according to the manufacturer's instructions. The protein concentrations were determined using a bicinchoninic acid protein assay (Thermo Fisher Scientific). Equal amount of each

protein sample were electrophoresed on sodium dodecyl sulfate-polyacrylamide gel electrophoresis (SDS-PAGE) and subsequently transferred to polyvinylidene fluoride (PVDF) membrane (Millipore, Burlington, MA, USA) at 4℃. Thereafter, the membrane was blocked using 5% BSA in Tris buffered saline with Tween 20 (TBS-T; Santa Cruz Biotechnology Inc., Dallas, TX, USA) for 1 h and incubated with the primary antibodies at 4℃ overnight, followed by incubated with secondary antibody (1 : 5000 dilution) for 1 h. The immunoreactive bands were visualized using the ECL System (Sigma Aldrich), exposed on MicorChemi 4.2 (Dong-Il Shimadzu Corp., Seoul, Korea). The antibody conditions used in this study are summarized in Table 1.

Ⅱ-9. Quantitative polymerase chain reaction (qPCR)

After 6 days induction with RANKL or 25-HC, total RNA was extracted using TRIzol reagent (Invitrogen, Waltham, CA, USA) according to the manufacturer's protocol. The concentration of total RNA was determined by the Nanodrop 2000 (Thermo Fisher Scientific). qPCR Bio cDNA synthesis kit (PCR Biosystems, London, UK) was used to synthesise cDNA according to the manufacturer's instructions. qPCR was performed using PCRBIO Taq DNA Polymerase kit (PCR Biosystems) and specific primers on a TaKaRa PCR Thermal Cycler Dice (TaKaRa Bio Inc.). Thereafter, the PCR products were electrophoresed on an agarose gel to determine the expression level of the target genes. Glyceraldehyde 3-phosphate dehydrogenase (GAPDH) was used as an internal control. The PCR primer conditions used in this study are summarized in Table 2.

Ⅱ-10. Immunocytochemistry

MDPC-23 cells were cultured at a density 1 × 10^3 cells/well on 8-well chamber slides, and then treated with 50, 100, and 200 nM of 25-HC or 50 ng/mL RANKL for

6 days. Thereafter, the cell were subjected to immunocytochemistry with primary antibodies (1 : 250 dilution) at 4℃ overnight and then incubated with Alexa 488-conjugated secondary antibodies (Thermo fisher Scientific, 1:500 dilution) in 4',6-Diamidino-2-phenylindole dihydrochloride (DAPI; Vector Laboratories, Inc., Burlingame, CA, USA) for 1 h. The cells were imaged using a laser confocal scanning microscope system (Leica Microsystems) and counted to plot the histogram.

Ⅱ-11. Gelatin zymography

Gelatin zymography was performed to assess the activation of matrix metalloproteinases (MMPs) in MDPC-23 cells. Briefly, the cells were treated with 50, 100, and 200 nM 25-HC or 50 ng/mL RANKL for 6 days. Thereafter, an equal volume of conditioned medium was electrophoresed on a 10% polyacrylamide gel containing copolymerized 4 mg/mL gelatin (Sigma-Aldrich). After electrophoresis, the gel was incubated in zymogram renaturing buffer [50 mM Tris-HCI (pH 7.6), 10 mM $CaCl_2$, 50 mM NaCl, and 0.05% Brij-35] at 37℃ for 24 h. After renaturation of MMPs, the gel was stained with 0.1% coomassie brilliant blue R250 (Merck, Darmstadt, Germany). Gelatinolytic bands were revealed as clear bands on a background stained light blue and then imaged using a digital camera.

Ⅱ-12. Dentine resorption assay

MDPC-23 cells (1×10^3 cells/well) were cultured on dentine discs (Immunodiagnostic Systems Inc., Gaithersburg, MD, USA) in a 96-well plate (SPL Life Science, Pocheon, Republic of Korea) with 50, 100, and 200 nM 25-HC or 50 ng/mL RANKL. After 6 days, the dentine discs were rinsed with sodium hypochlorite (NaOCl; Sigma-Aldrich) for 5 min. The dentine discs were stained with 1% toluidine blue O (Sigma-Aldrich) in

0.5% soduim tetraborate (Sigma-Aldrich) for 1 min. Then, the resorption pits were observed with microscopy Leica DM750 microscope.

Ⅱ-13. Measurement of prostaglandin E_2 (PGE_2) Production

MDPC-23 cells were seed at 1×10^5 cells/well in a 6-well culture plate. The cells were treated with 0, 50, 100, and 200 nM 25-HC or 50 ng/mL RANKL. The production of PGE_2 was measured using a Parameter™ PGE_2 assay kit (R&D systems, inc., minneapolis, MN, USA), according to manufacturer's protocol. The supernatant was collected on 6 days. The levels of PGE_2 were assessed by a spectrophotometer at 450 nm and normalized with the standard solution.

Ⅱ-14. Statistical analysis

The experimental data were presented as the mean ± standard deviation and were compared using analysis of variance, followed by post-hoc multiple comparison (Tukey's test) using SPSS software version 22 (IBM Corp.). $p<0.05$ was considered to indicate statistically significant differences. All the data were obtained from three independent experiments.

Ⅲ. RESULTS

Ⅲ-1. CH25H upregulates the synthesis of 25-HC in lipopolysaccharide (LPS)-treated MDPC-23 cells

To determine the effect of inflammatory conditions on 25-HC synthesis, MDPC-23 cells were cultured in the presence of 0.1 and 1 μg/mL LPS. Next, total RNA and total proteins were extracted from the cells using TRIzol reagent and cell lysis buffer, respectively, at day 6 post-treatment. As shown in Figure 2A–B, LPS upregulated the mRNA and protein levels of CH25H in MDPC-23 cells. Furthermore, the production of 25-HC in MDPC-23 cells treated with 0.1 (156.9 ± 8.9 pmol/mL) and 1 μg/mL LPS (171.5 ± 6.6 pmol/mL) for 6 days was significantly higher than that in control MDPC-23 cells (123.2 ± 4.4 pmol/mL; Figure 2C). These findings indicate that LPS promotes the synthesis of 25-HC, an oxysterol synthesized from cholesterol, by upregulating CH25H in MDPC-23 cells

Ⅲ-2. 25-HC does not affect the viability of MDPC-23 cells

The CCK-8 assay was performed to investigate the effect of 25-HC on the viability of MDPC-23 cells. As shown in Figure 3A, the percentage viabilities of MDPC-23 cells on day 2 post-treatment with 50, 100, and 200 nM of 25-HC were 101.9 ± 1.5%, 97.0 ± 1.6%, and 96.3 ± 3.7%, respectively, when compared with those of control MDPC-23 cells (100.0 ± 1.8%). At day 4 post-treatment, the percentage viabilities of MDPC-23 cells treated with 50, 100, and 200 nM of 25-HC were 193.85 ± 3.9, 200.2 ± 2.8%, and 220.3 ± 4.4%, respectively, when compared with those of control MDPC-23 cells (191.3 ± 2.6%; Figure 3A). The percentage viabilities of MDPC-23 cells treated with 50, 100, and 200 nM of 25-HC were 295.8 ± 7.7%, 287.8 ± 4%, and 309.4 ± 4.9%, respectively, when compared with those of control MDPC-23 cells

(269.7 ± 5.1%; Figure 3A) on day 6 post-treatment. Viability staining was performed to verify the effect of 25-HC on the proliferation of MDPC-23 cells. The live cells were stained with green calcein AM (green fluorescence), whereas the dead cells were stained with ethidium homodimer-1 (red fluorescence). Consistent with the results of the CCK-8 assay, the number of cells exhibiting green fluorescence (live cells) was high in the group treated with 50–200 nM of 25-HC for 2, 4, and 6 days. These findings indicated that 25-HC did not affect the viability of MDPC-23 cells.

Ⅲ-3. 25-HC induces the odontoclastogenesis of MDPC-23 cells

H&E staining and TRAP assay were performed to investigate the ability of 25-HC to induce odontoclastogenesis in MDPC-23 cells. MDPC-23 cells were cultured with 25-HC (50 – 200 nM) or RANKL (50 ng/mL; positive control; induces odontoclastogenesis) for 6 days. The morphology of multinucleated cells and TRAP-positive odontoclasts was analyzed using H&E staining and TRAP assay, respectively. As shown in Figure 4A, the results of H&E staining revealed that treatment with RANKL or 50 – 200 nM of 25-HC for 6 days promoted the formation of multinucleated MDPC-23 cells (Figure 4A). Moreover, the number of multinucleated cells in the groups treated with 50 – 200 nM of 25-HC was significantly higher than that in the group treated with 50 ng/mL RANKL (Figure 4A). As shown in Figure 4B, treatment with RANKL or 25-HC increased the number of TRAP positive MDPC-23 cells. However, the intensity of TRAP staining in MDPC-23 cells treated with 50 – 200 nM of 25-HC was higher than that in MDPC-23 cells treated with RANKL. As shown in Figure 4C, the proportion of TRAP positive cells among MDPC-23 cells treated with 50, 100, and 200 nM of 25-HC was 5.6 ± 0.9%, 7.2 ± 0.7%, and 15.4 ± 3.1%, respectively, when compared with that among control MDPC-23 cells (1.3 ± 0.7%). Additionally, the number of TRAP positive cells in the groups treated with 100 and 200 nM of 25-HC was significantly higher than that in the group treated with RANKL (3.7 ± 0.1%; Figure 4C). Furthermore, the activity of TRAP in MDPC-23

cells treated with RANKL or 25-HC was higher than that in control MDPC-23 cells (Figure 4D). These findings indicate that 25-HC promotes odontoclastogenesis in odontoblast-like MDPC-23 cells.

Ⅲ-4. 25-HC accelerates dentin resorption in MDPC-23 cells through the upregulation of MMP-2 and MMP-9

To examine if the multinucleated cells obtained from 25-HC-mediated differentiation of MDPC-23 cells induce dentin resorption, MDPC-23 cells were cultured on dentin discs in the presence of 50 ng/mL RANKL or 50, 100, and 200 nM of 25-HC for 6 days. The dentin discs were rinsed with NaOCl and stained with toluidine blue O in 0.5% sodium tetraborate. As shown in Figure 5, the dentin resorption pit was not significantly different between RANKL (50 ng/mL)-treated, 25-HC (50 mM)-treated, and control MDPC-23 cells. In contrast, treatment with 100 or 200 nM of 25-HC markedly increased the formation of dentin resorption lacunae (Figure 5). Furthermore, the expression and activity of dentin resorption-associated enzymes, such as MMP-2 and MMP-9 were examined. MDPC-23 cells were treated with 50 ng/mL RANKL or 50, 100, and 200 nM of 25-HC for 6 days. The conditioned media were subjected to SDS-PAGE and gelatin zymography to investigate the activation and expression of MMP-2 and MMP-9, respectively. As shown in Figure 6A–B, the expression and activation of MMP-2 and MMP-9 in the 25-HC-treated group were significantly upregulated when compared with those in the RANKL treated and control groups. These findings indicate that 25-HC promotes dentin resorption in MDPC-23 cells by upregulating the expression and activation of MMP-2 and MMP-9 during odontoclast differentiation.

Ⅲ-5. 25-HC promotes odontoclastogenesis through the nuclear translocation of NF-κB-NFATc1 from the cytosol in MDPC-23 cells

To confirm 25-HC-induced odontoclastogenesis, the effect of 50 ng/mL RANKL or 50 - 200 nM of 25-HC treatment for 6 days on the odontoclastogenesis-associated proteins was investigated using western blotting. The phosphorylation of NF-κB in 25-HC-treated MDPC-23 cells was significantly higher than that in RANKL-treated and control MDPC-23 cells (Figure 7A). The expression levels of NF-κB downstream molecules, such as tumor necrosis factor receptor associated factors 6 (TRAF6), NFATc1, c-fos and cathepsin K were significantly upregulated in the 25-HC-treated MDPC-23 cells (Figure 7A). Phosphorylated NF-κB undergoes nuclear translocation from the cytosol and initiates the expression of odontoclastogenesis-associated proteins. Thus, the effect of treatment with 50 ng/mL RANKL or 50, 100, and 200 nM of 25-HC for 6 days on the cytosolic and nuclear proteins was examined in MDPC-23 cells. As shown in Figure 7B, the expression levels of NF-κB and its downstream transcription factor NFATc1 were significantly downregulated in the cytosolic fraction of 25-HC-treated MDPC-23 cells during odontoclastogenesis. In contrast, 25-HC upregulated the expression levels of NF-κB and NFATc1 in the nuclear fraction of MDPC-23 cells (Figure 7B). These findings indicate that 25-HC induces odontoclastogenesis of MDPC-23 cells by promoting the nuclear translocation of NF-κB and NFATc1 from the cytosol.

Ⅲ-6. 25-HC induces odontoclastogenesis in MDPC-23 cells by upregulating RANKL

To investigate the cellular mechanism underlying 25-HC-induced odontoclastogenesis the effect of treatment with 50 ng/mL RANKL or 50, 100, and 200 nM of 25-HC for 6 days on the expression levels of RANKL and its receptors RANK and osteoprotegerin (OPG) were examined using western blotting and immunocytochemical

analyses. As shown in Figure 8A, the expression levels of RANKL and RANK in 25-HC-treated MDPC-23 cells were upregulated when compared with those in control MDPC-23 cells. In contrast, the expression levels of OPG were downregulated in 25-HC-treated MDPC-23 cells. Immunocytochemical analysis revealed that the expression levels of RANKL were significantly upregulated in 25-HC-treated MDPC-23 cells during odontoclastogenesis (Figure 8B). These findings suggest that 25-HC induces odontoclastogenesis in MDPC-23 cells by upregulating the expression of RANKL-RANK and downregulating the expression of OPG.

Ⅲ-7. 25-HC induces the production of ROS in MDPC-23 cells through the Rac1/2/3-nicotinamide adenine dinucleotide phosphate oxidase 1 (NOXO1) axis

ROS are key odontoclastogenesis-inducing factors [21]. Therefore, the effect of treatment with 50 – 200 nM of 25-HC or 50 ng/mL RANKL on the production of ROS during odontoclastogenesis in MDPC-23 cells was examined using H2DCF-DA staining. As shown in Figure 9A–B, treatment with 50 ng/mL RANKL slightly increased the ROS levels, whereas treatment with 50, 100, and 200 nM of 25-HC markedly increased the ROS levels in MDPC-23 cells. Furthermore, the production of intracellular ROS is associated with NOXO1 and Rac1 [22]. Hence, the effects of treatment with 50 ng/mL RANKL or 50–200 nM of 25-HC for 6 days on the levels of Rac1/2/3 and NOXO1 were examined using western blotting. As shown in Figure 9C, the expression levels of NOXO1 and Rac1/2/3 in 25-HC (100 or 200 nM)-treated MDPC-23 cells were significantly upregulated when compared with those in RANKL-treated and control MDPC-23 cells. These findings suggest that 25-HC induces odontoclastogenesis in MDPC-23 cells by upregulating ROS production through the NOXO1-Rac1/2/3 axis.

Ⅲ-8. 25-HC upregulates the expression of inflammatory mediators and pro-inflammatory cytokines in MDPC-23 cells through the modulation of the nuclear factor erythroid-2-related factor 2 (Nrf2)-heme oxygenase-1 (HO-1) axis

Western blotting was performed to investigate the role of 25-HC-induced ROS production in upregulating the expression of inflammatory mediators in MDPC-23 cells. As shown in Figure 10A, the expression levels of inducible nitric oxide synthase (iNOS) and cyclooxygenase-2 (COX-2) in 25-HC-treated MDPC-23 cells were significantly upregulated when compared with those in RANKL-treated and control MDPC-23 cells. Furthermore, the levels of PGE_2 in cell culture supernatant were examined using enzyme-linked immunosorbent assay (ELISA). The levels of PGE_2 in the culture supernatant of MDPC-23 cells treated with 50 (1187.2 ± 46.4 pg/mL), 100 (1435.2 ± 56.7 pg/mL), and 200 nM (1493.6 ± 59.1 pg/mL) of 25-HC were significantly higher than those in the culture supernatant of control MDPC-23 cells (940.5 ± 36.4 pg/mL, Figure 10B). Moreover, the expression levels of pro-inflammatory cytokines, such as tumor necrosis factor-α (TNF-α) and interleukin-6 (IL-6), which are closely associated with clastogenesis of osteoclasts and odontoclasts, were significantly upregulated in 25-HC-treated MDPC-23 cells (Figure 10C). Nrf2 and HO-1 are reported to be closely associated with the regulation of inflammation [23]. Western blotting analysis revealed that the expression levels of Nrf2 and its downstream regulator HO-1 were significantly downregulated in 25-HC-treated MDPC-23 cells (Figure 10D). These findings indicate that 25-HC upregulates the expression of inflammatory mediators and pro-inflammatory cytokines in MDPC-23 cells through the modulation of the Nrf2/HO-1 axis.

Ⅲ-9. 25-HC induces odontoclastogenesis in MDPC-23 cells through the activation of the NF-κB cellular signaling pathway

CDDO-Me is a Nrf2 activator and an NF-κB pathway inhibitor [24-25]. To investigate the effects of CDDO-Me on 25-HC-induced odontoclast differentiation, MDPC-23 cells were treated with 50 ng/mL RANKL or 200 nM of 25-HC in the absence or presence of 50 nM CDDO-Me for 6 days. As shown in Figure 11A, RANKL and 25-HC promoted the differentiation of MDPC-23 cells into mature TRAP-positive multinucleated cells in the absence of CDDO-Me. In contrast, treatment with CDDO-Me decreased the formation and number of TRAP-positive multinucleated cells in the RANKL-treated and 25-HC-treated groups (Figure 11A). The number of TRAP positive cells in the RANKL (50 ng/mL)-treated and 25-HC (200 nM)-treated groups was significantly higher than that in the control group. However, treatment with CDDO-Me decreased the number of TRAP positive cells (Figure 11B). Additionally, CDDO-Me significantly decreased the number of TRAP positive cells in RANKL-treated and 25-HC-treated MDPC-23 cells (Figure 11B). As shown in Figure 11C, TRAP activity was significantly upregulated in RANKL-treated and 25-HC-treated MDPC-23 cells. However, CDDO-Me mitigated the RANKL-induced and 25-HC-induced upregulation of TRAP-activity in MDPC-23 cells (Figure 11C). These findings indicate that the NF-κB antagonist CDDO-Me inhibits the differentiation of odontoclast from 25-HC-treated MDPC-23 cells. Next, the effect of CDDO-Me on the expression levels of odontoclastogenesis-related factors in RANKL-treated and 25-HC-treated MDPC-23 cells was examined using western blotting. As shown in Figure 12A, treatment with CDDO-Me significantly mitigated the RANKL-induced and 25-HC-induced upregulation of odontoclastogenesis-related biomarkers, such as TRAF6, NF-κB, NFATc1, cathepsin K, and downregulation of c-fos in MDPC-23 cells. Furthermore, treatment with CDDO-Me significantly downregulated the expression levels of odontoclast differentiation-related factors, in RANKL-treated and 25-HC-treated MDPC-23 (Figure 12B). However, the expression levels of OPG were upregulated in RANKL-treated and 25-HC-treated MDPC-23 cells upon treatment with CDDO-Me (Figure 12B). These

findings indicate that the inhibition of NF-κB suppresses the expression of odontoclastogenesis-related factors in 25-HC-treated MDPC-23 cells. As shown in Figure 13A, CDDO-Me suppressed the nuclear translocation of NF-κB in RANKL-treated and 25-HC-treated MDPC-23 cells. Moreover, nuclear translocation of NF-κB was observed in the multinucleated cells differentiated from RANKL-treated and 25-HC-treated MDPC-23 (Figure 13B). In contrast, multinucleated cells were not observed in RANKL-treated and 25-HC-treated MDPC-23 cells upon treatment with CDDO-Me, which suppressed NF-κB nuclear translocation (Figure 13B). These findings indicate that 25-HC induces odontoclastogenesis in MDPC-23 cells by activating the NF-κB cellular signaling pathway in MDPC-23 cells.

Ⅳ. DISCUSSION

Internal tooth resorption, which is predominantly a lesion within the upper third region of the pulp chamber, may affect both the crown and root of the tooth [26]. The initiation of internal tooth resorption occurs in the inner wall of the root canal and progresses in a centrifugal direction [26]. Internal tooth resorption can sometimes be accompanied by resorption of the root surface or alveolar bone [26]. Hence, internal tooth resorption can only be diagnosed when external factors, including root caries or cervical resorption, can be excluded [26]. Previous studies have reported the radiological and histological characteristics of internal tooth resorption. However, the correlation between external and internal root resorption is unclear [26]. Additionally, external tooth resorption mediated by trauma, ectopic teeth, or orthodontic tooth movement may affect approximately 5% of all permanent teeth [27]. Internal tooth resorption, a rare condition, is closely associated with an inflammatory condition that induces the progressive degeneration of intraradicular dentin and dental tubules along the middle and apical canal walls [28]. However, the pathophysiological etiology of internal tooth resorption has not been completely elucidated [26].

Odontoclast is a multinucleated dental tissue-localized hard tissue-resorbing cell derived from circulating progenitor cells, such as monocytes/macrophages residing in the dental pulp and periodontal ligament through the secretion of colony stimulating factor 1, RANKL and OPG [10]. Similar to osteoclasts, odontoclasts express TRAP, cathepsin K, and MMPs, such as MMP-9 [8,29]. Although odontoclasts are generally associated with the physiological root resorption of primary dentition before exfoliation, odontoclasts induce odontoclastic root resorption of permanent teeth under pathological conditions, such as inflammation [8]. Hence, the increase in the number of odontoclast with characteristics similar to those of osteoclasts may accelerate the odontoclastic internal root resorption. However, the regulation of odontoclastogenesis is not completely understood.

Recent studies have suggested a pathophysiological link between metabolic syndrome and periodontal diseases [30-34]. Metabolic syndrome is characterized by dyslipidemia,

hypertension, obesity, and dysglycemia, which are closely associated with lipid and cholesterol metabolism [32]. Recent studies have reported that metabolic syndromes induce chronic low-grade inflammation, which may be a pathophysiological factor for periodontal disease [35-36]. Metabolic syndrome-induced chronic low-grade inflammation is closely associated with the synthesis of oxysterols, which are cholesterol derivatives synthesized through cholesterol oxidation via the enzymatic and non-enzymatic pathways. Oxysterols are involved in several physiological functions at very low concentrations. However, some oxysterols are involved in the pathogenesis of several human diseases, including periodontal diseases. Recent studies have demonstrated that 27-hydroxycholesterol and 7-ketocholesterol promoted osteoclastogenesis [37-38]. In particular, Zhang et al. reported that 25-HC, which is synthesized from cholesterol through CH25H activity, promoted RANKL-induced osteoclastogenesis [20]. Hence, these studies demonstrate that metabolic syndrome-induced oxysterols may be associated with the differentiation of hard tissue-resorbing cells. Additionally, Li et al. have reported that LPS promoted odontoclastogenesis in mouse papilla-derived MDPC-23 cells [39]. LPS, an outer membrane component of gram-negative bacteria, induces the production of pro-inflammatory cytokines [39]. Furthermore, LPS promotes the differentiation of osteoclasts through the activation of interleukin-1, TNF-α and RANKL [40-42]. Thus, this study hypothesized that inflammation-induced oxysterols are involved in odontoclastogenesis. In this study, the expression of CH25H was upregulated in LPS-treated MDPC-23 cells (Figure 2A–B). Furthermore, the production of 25-HC was significantly upregulated in LPS-treated MDPC-23 cells (Figure 2C). Previous studies have reported that the expression of CH25H is significantly upregulated in the adipose tissue, articular cartilage, and lung under inflammatory conditions [43-45]. Although the biological link between 25-HC and inflammation is unclear, recent studies have reported that 25-HC contributes to inflammation [46-47]. Hence, the findings of previous studies and this study suggest that the oxysterol 25-HC is upregulated in odontoblast-like MDPC-23 cells under inflammatory conditions.

Recently, some oxysterols were reported to induce oxiapoptophagy, which is a type of cell death characterized by oxidative stress, apoptosis, and autophagy [48]. Hence, the effects of 25-HC on the viability and survival of MDPC-23 cells during the

differentiation period were examined. As shown in Figure 3, treatment with 50 − 200 nM of 25-HC for 6 days did not affect the viability of MDPC-23 cells. Next, the effect of treatment with 50 − 200 nM of 25-HC for 6 days on odontoclastogenesis in MDPC-23 cells was investigated. Similar to osteoclasts, the odontoclasts are multinucleated cells [39]. In this study, 25-HC increased the number of multinucleated cells and upregulated TRAP expression in MDPC-23 cells (Figure 4). Moreover, the odontoclast is a dental tissue-localized hard tissue-resorbing cell with upregulated expression of MMPs [10]. Treatment with 25-HC significantly increased dentin resorption in MDPC-23 cells cultured on dentin discs by upregulating the expression and activation of MMP-2 and MMP-9 (Figures 5&6). During differentiation, the expression of TRAF6 was significantly upregulated in 25-HC-treated MDPC-23 cells (Figure 7). Treatment with 25-HC promoted the formation of the TRAF6-NF-κB-axis-mediated NFATc-1-c-fos complex, which is a cellular signaling pathway associated with osteoclast differentiation and resorption gene induction in MDPC-23 cells. Additionally, MDPC-23 upregulated the expression of cathepsin K, which is an osteoclast/odontoclast biomarker (Figure 7). These results indicate that 25-HC induces odontoclastogenesis in MDPC-23 cells.

Osteoclastogenesis is regulated by the RANKL-RANK-OPG axis [49]. RANKL initiates osteoclast differentiation by binding to its receptor RANK [50]. Osteoclastogenesis is initiated by the upregulation of TRAF6 which leads to the phosphorylation of NF-κB, NFATc1, and c-fos [50-52]. Additionally, OPG, a soluble receptor for RANKL, inhibits osteoclastogenesis by binding to RANKL [53]. In this study, 25-HC significantly upregulated the expression of TRAF6, a downstream target of the RANKL-RANK signaling axis, during odontoclastogenesis in MDPC-23 cells (Figure 7A). Hence, this study hypothesized that 25-HC-induced odontoclastogenesis involves RANKL in MDPC-23 cells. As shown in Figure 8, the expression levels of RANKL and RANK were significantly upregulated in 25-HC-treated MDPC-23 cells. In contrast, 25-HC downregulated OPG expression (Figure 8). These results indicate that 25-HC accelerates odontoclastogenesis by increasing the binding of RANKL-RANK.

Ha et al. reported that RANKL stimulated the production of ROS, which are cellular secondary messengers, in osteoclasts [54]. ROS, including O_2^- and H_2O_2, are associated

with bone homeostasis and osteoclast differentiation through the upregulation of inflammation [55-56]. Furthermore, ROS promotes osteoclastic bone resorption and osteoclastogenesis through the activation of mitogen-activated protein kinases [23,54]. Hence, the inhibition of ROS is considered a potential therapeutic strategy for the prevention of ROS-mediated osteoclasts diseases [55]. Previous studies have reported that 25-HC significantly increased the production of ROS in various types of cells, such as human retinal cells [57], human umbilical vascular endothelial cells [58], rat pheochromocytoma PC12 [59], and primary porcine retinal pigment epithelial cells [60]. This study hypothesized that 25-HC-induced RANKL increases ROS production during odontoclastogenesis in MDPC-23 cells. As shown in Figure 9, ROS production was significantly upregulated in 25-HC-treated MDCP-23 cells during odontoclastogenesis.

Rac1, a Rho GTP enzyme subfamily member and a component of the nicotinamide adenine dinucleotide phosphate (NADPH) oxidase complex, is expressed in monocytes/macrophages and plays a critical role in the production of ROS [39,61]. The NADPH oxidase holoenzyme comprises transmembrane catalytic cell type-specific Nox subunits 1−5, the transmembrane p22phox protein, and cofactors, including NOX1, NOXA1, p67phox, and p47phox. Rac1 binds to NOXA1 of the NADPH oxidase complex to initiate ROS production [62-63]. The expression levels of Rac1/2/3 and NOXO1 were significantly upregulated in 25-HC-treated MDPC-23 cells (Figure 9). These data findings that 25-HC-induced RANKL upregulation is accompanied by enhanced ROS production mediated by NAPDH oxidase through the Rac1-NOXO1 cellular signaling axis during odontoclastogenesis in MDPC-23 cells.

Inflammation is accompanied by the enhanced production of ROS [64]. Wong et al. reported that 25-HC promotes the production of IL-1β, which is a representative pro-inflammatory cytokine, in microglial cells [47]. Hence, 25-HC was hypothesized to upregulate the expression of inflammatory mediators and inflammatory cytokines in MDPC-23 cells. As shown in Figure 10, inflammatory mediators, such as iNOS, COX-2, and PGE_2 were significantly upregulated in MDPC-23 cells. Treatment with 25-HC significantly upregulated the expression of pro-inflammatory cytokines, such as TNF-α and IL-6 in MDPC-23 cells. Fujihara et al. reported that TNF-α upregulated the expression of RANKL in gingival epithelial cells [65-66]. Zhang et al. reported that

TNF-α stimulated RANKL-induced osteoclastogenesis through the TNF type I receptor and the RANK signaling pathway [67]. IL-6 is closely associated with osteoclastogenesis [68]. Wu et al. reported that IL-6 promoted osteocyte-mediated osteoclastogenesis through the upregulation of JAK2 and RANKL activity [69]. Kudo et al. reported that IL-6 supported the formation of human osteoclasts through a RANKL-independent mechanism [70]. These findings suggest that 25-HC-induced odontoclastogenesis is associated with the production of pro-inflammatory cytokines, such as TNF-α and IL-6 in MDCP-23 cells.

As shown in Figure 10D, 25-HC downregulated the expression of Nrf2 and HO-1 in MDPC-23 cells. Previous studies have revealed that the transcription factor Nrf2 exerts cytoprotective effects by regulating the expression of phase II detoxifying enzymes, such as NADPH, HO-1, and antioxidant genes [71-73]. Kanzaki et al. reported that RANKL attenuated Nrf2-mediated antioxidant enzyme expression [74]. Hence, the activation of Nrf2 attenuated RANKL-induced osteoclastogenesis by inhibiting NF-κB phosphorylation [75-76]. HO-1 plays an important role in inflammation [77]. The expression of HO-1 mitigates inflammation through the catalytic breakdown of heme, which is an iron-containing tetrapyrrole complex with pro-inflammatory effects [77]. Bak et al. reported that the upregulation of HO-1 suppressed the RANKL-induced osteoclastogenesis by inhibiting NF-κB phosphorylation [78]. These findings demonstrate that 25-HC promotes odontoclastogenesis in MDPC-23 cells by upregulating inflammation through the Nrf2-HO-1 axis.

However, RANKL-induced osteoclastogenesis and odontoclastogenesis are initiated by the phosphorylation of NF-κB in monocytes/macrophages [79]. Previous studies have revealed that the Nrf2-HO-1 axis suppresses RANKL-induced osteoclastogenesis by downregulating NF-κB phosphorylation [78,80]. Hence, this study hypothesized that the inhibition of the NF-κB cellular signaling pathway suppresses odontoclastogenesis in 25-HC-treated MDPC-23 cells. As shown in Figures 11−13, CDDO-Me, a Nrf2 activator and an inhibitor of the NF-κB pathway, suppressed odontoclastogenesis in 25-HC-treated MDPC-23 cells. These findings indicate that 25-HC-mediated odontoclastogenesis in MDPC-23 cells is mediated through the upregulation of RANKL which initiates the NF-κB cellular signaling pathways, and the modulation of the Nrf2-HO-1 axis.

In conclusion, this study demonstrated that 25-HC induces odontoclastogenesis in MDPC-23 cells by upregulating RANKL, downregulating OPG, and promoting the production of inflammation and ROS. The upregulation of 25-HC may function as a pathophysiological risk factor to accelerate internal tooth resorption by promoting odontoclastogenesis (Figure 14). Therefore, the findings of this study suggest that metabolic syndrome may be a pathophysiological etiological factor for internal tooth resorption.

Ⅴ. REFERENCES

[1] Pollanen MT, Salonen JI, Uitto VJ. Structure and function of the tooth-epithelial interface in health and disease. Periodontol 2000. 2003;31:12-31.

[2] Goldberg M, Kulkarni AB, Young M, Boskey A. Dentin: structure, composition and mineralization. Front Biosci (Elite Ed). 2011;3:711-35.

[3] Cordeiro MM, Dong Z, Kaneko T, Zhang Z, Miyazawa M, Shi S, et al. Dental pulp tissue engineering with stem cells from exfoliated deciduous teeth. J Endod. 2008;34(8):962-9.

[4] Charadram N, Farahani RM, Harty D, Rathsam C, Swain MV, Hunter N. Regulation of reactionary dentin formation by odontoblasts in response to polymicrobial invasion of dentin matrix. Bone. 2012;50(1):265-75.

[5] Kawai T, Akira S. The role of pattern-recognition receptors in innate immunity: update on Toll-like receptors. Nat Immunol. 2010;11(5):373-84.

[6] Beutler B. Microbe sensing, positive feedback loops, and the pathogenesis of inflammatory diseases. Immunol Rev. 2009;227(1):248-63.

[7] Lee K, Lee BM, Park CK, Kim YH, Chung G. Ion Channels Involved in Tooth Pain. Int J Mol Sci. 2019;20(9).

[8] Kamat M, Puranik R, Vanaki S, Kamat S. An insight into the regulatory mechanisms of cells involved in resorption of dental hard tissues. J Oral Maxillofac Pathol. 2013;17(2):228-33.

[9] Sasaki T. Differentiation and functions of osteoclasts and odontoclasts in mineralized tissue resorption. Microsc Res Tech. 2003;61(6):483-95.

[10] Wang Z, McCauley LK. Osteoclasts and odontoclasts: signaling pathways to development and disease. Oral Dis. 2011;17(2):129-42.

[11] Oshiro T, Shibasaki Y, Martin TJ, Sasaki T. Immunolocalization of vacuolar-type H+-ATPase, cathepsin K, matrix metalloproteinase-9, and receptor activator of NFkappaB ligand in odontoclasts during physiological root resorption of human deciduous teeth. Anat Rec. 2001;264(3):305-11.

[12] Hanks CT, Sun ZL, Fang DN, Edwards CA, Wataha JC, Ritchie HH, et al.

Cloned 3T6 cell line from CD-1 mouse fetal molar dental papillae. Connect Tissue Res. 1998;37(3-4):233-49.

[13] Duan X, Yang T, Zhang Y, Wen X, Xue Y, Zhou M. Odontoblast-like MDPC-23 cells function as odontoclasts with RANKL/M-CSF induction. Arch Oral Biol. 2013;58(3):272-8.

[14] Bauman DR, Bitmansour AD, McDonald JG, Thompson BM, Liang G, Russell DW. 25-Hydroxycholesterol secreted by macrophages in response to Toll-like receptor activation suppresses immunoglobulin A production. Proc Natl Acad Sci U S A. 2009;106(39):16764-9.

[15] Park K, Scott AL. Cholesterol 25-hydroxylase production by dendritic cells and macrophages is regulated by type I interferons. J Leukoc Biol. 2010;88(6):1081-7.

[16] Cyster JG, Dang EV, Reboldi A, Yi T. 25-Hydroxycholesterols in innate and adaptive immunity. Nat Rev Immunol. 2014;14(11):731-43.

[17] Gold ES, Ramsey SA, Sartain MJ, Selinummi J, Podolsky I, Rodriguez DJ, et al. ATF3 protects against atherosclerosis by suppressing 25-hydroxycholesterol-induced lipid body formation. J Exp Med. 2012;209(4):807-17.

[18] Gold ES, Diercks AH, Podolsky I, Podyminogin RL, Askovich PS, Treuting PM, et al. 25-Hydroxycholesterol acts as an amplifier of inflammatory signaling. Proc Natl Acad Sci U S A. 2014;111(29):10666-71.

[19] Trindade BC, Ceglia S, Berthelette A, Raso F, Howley K, Muppidi JR, et al. The cholesterol metabolite 25-hydroxycholesterol restrains the transcriptional regulator SREBP2 and limits intestinal IgA plasma cell differentiation. Immunity. 2021; 54(10):2273-87 e6.

[20] Zhang L, Lv Y, Xian G, Lin Y. 25-hydroxycholesterol promotes RANKL-induced osteoclastogenesis through coordinating NFATc1 and Sp1 complex in the transcription of miR-139-5p. Biochem Biophys Res Commun. 2017;485(4):736-41.

[21] Lee NK, Choi YG, Baik JY, Han SY, Jeong DW, Bae YS, et al. A crucial role for reactive oxygen species in RANKL-induced osteoclast differentiation. Blood. 2005;106(3):852-9.

[22] Cheng G, Diebold BA, Hughes Y, Lambeth JD. Nox1-dependent reactive oxygen generation is regulated by Rac1. J Biol Chem. 2006;281(26):17718-26.

[23] Loboda A, Damulewicz M, Pyza E, Jozkowicz A, Dulak J. Role of Nrf2/HO-1 system in development, oxidative stress response and diseases: an evolutionarily conserved mechanism. Cell Mol Life Sci. 2016;73(17):3221-47.

[24] Kawashima N, Okiji T. Odontoblasts: Specialized hard-tissue-forming cells in the dentin-pulp complex. Congenit Anom (Kyoto). 2016;56(4):144-53.

[25] Bleicher F. Odontoblast physiology. Exp Cell Res. 2014;325(2):65-71.

[26] Koehne T, Zustin J, Amling M, Friedrich RE. Radiological and Histopathological Features of Internal Tooth Resorption. In Vivo. 2020;34(4):1875-82.

[27] Weltman B, Vig KW, Fields HW, Shanker S, Kaizar EE. Root resorption associated with orthodontic tooth movement: a systematic review. Am J Orthod Dentofacial Orthop. 2010;137(4):462-76; discussion 12A.

[28] Patel S, Ricucci D, Durak C, Tay F. Internal root resorption: a review. J Endod. 2010;36(7):1107-21.

[29] Nishida D, Arai A, Zhao L, Yang M, Nakamichi Y, Horibe K, et al. RANKL/OPG ratio regulates odontoclastogenesis in damaged dental pulp. Sci Rep. 2021;11(1):4575.

[30] Srivastava MC, Srivastava R, Verma PK, Gautam A. Metabolic syndrome and periodontal disease: An overview for physicians. J Family Med Prim Care. 2019; 8(11):3492-5.

[31] Bandiwadekar AS, Shanbhag N, Madhuniranjanswamy MS, Khanagar SB, Naik S, Siddeeqh S. Association of Periodontitis With Metabolic Syndrome: A Case-Control Study. J Int Soc Prev Community Dent. 2020;10(4):458-65.

[32] Jepsen S, Suvan J, Deschner J. The association of periodontal diseases with metabolic syndrome and obesity. Periodontol 2000. 2020;83(1):125-53.

[33] Nascimento GG, Leite FRM, Peres KG, Demarco FF, Correa MB, Peres MA. Metabolic syndrome and periodontitis: A structural equation modeling approach. J Periodontol. 2019;90(6):655-62.

[34] Daudt LD, Musskopf ML, Mendez M, Remonti LLR, Leitao CB, Gross JL, et al. Association between metabolic syndrome and periodontitis: a systematic review and meta-analysis. Braz Oral Res. 2018;32:e35.

[35] Monteiro R, Azevedo I. Chronic inflammation in obesity and the metabolic syndrome. Mediators Inflamm. 2010;2010.

[36] Esser N, Legrand-Poels S, Piette J, Scheen AJ, Paquot N. Inflammation as a link between obesity, metabolic syndrome and type 2 diabetes. Diabetes Res Clin Pract. 2014;105(2):141-50.

[37] Zhang L, Liu M, Liu J, Li X, Yang M, Su B, et al. 27-Hydroxycholesterol enhanced osteoclastogenesis in lung adenocarcinoma microenvironment. J Cell Physiol. 2019;234(8):12692-700.

[38] Sul OJ, Li G, Kim JE, Kim ES, Choi HS. 7-ketocholesterol enhances autophagy via the ROS-TFEB signaling pathway in osteoclasts. J Nutr Biochem. 2021;96:108783.

[39] Li C, Qi WT, Jiang HW. Odontoclastogenesis of mouse papilla-derived MDPC-23 cells induced by lipopolysaccharide. Int Endod J. 2018;51 Suppl 2:e115-e24.

[40] Suda K, Woo JT, Takami M, Sexton PM, Nagai K. Lipopolysaccharide supports survival and fusion of preosteoclasts independent of TNF-alpha, IL-1, and RANKL. J Cell Physiol. 2002;190(1):101-8.

[41] Itoh K, Udagawa N, Kobayashi K, Suda K, Li X, Takami M, et al. Lipopolysaccharide promotes the survival of osteoclasts via Toll-like receptor 4, but cytokine production of osteoclasts in response to lipopolysaccharide is different from that of macrophages. J Immunol. 2003;170(7):3688-95.

[42] Inubushi T, Kawazoe A, Miyauchi M, Kudo Y, Ao M, Ishikado A, et al. Molecular mechanisms of the inhibitory effects of bovine lactoferrin on lipopolysaccharide-mediated osteoclastogenesis. J Biol Chem. 2012;287(28):23527-36.

[43] Russo L, Muir L, Geletka L, Delproposto J, Baker N, Flesher C, et al. Cholesterol 25-hydroxylase (CH25H) as a promoter of adipose tissue inflammation in obesity and diabetes. Mol Metab. 2020;39:100983.

[44] Choi WS, Lee G, Song WH, Koh JT, Yang J, Kwak JS, et al. The CH25H-CYP7B1-RORalpha axis of cholesterol metabolism regulates osteoarthritis. Nature. 2019;566(7743):254-8.

[45] Madenspacher JH, Morrell ED, Gowdy KM, McDonald JG, Thompson BM, Muse G, et al. Cholesterol 25-hydroxylase promotes efferocytosis and resolution of lung inflammation. JCI Insight. 2020;5(11).

[46] Jang J, Park S, Jin Hur H, Cho HJ, Hwang I, Pyo Kang Y, et al. 25-hydroxycholesterol contributes to cerebral inflammation of X-linked

adrenoleukodystrophy through activation of the NLRP3 inflammasome. Nat Commun. 2016;7:13129.

[47] Wong MY, Lewis M, Doherty JJ, Shi Y, Cashikar AG, Amelianchik A, et al. 25-Hydroxycholesterol amplifies microglial IL-1beta production in an apoE isoform-dependent manner. J Neuroinflammation. 2020;17(1):192.

[48] Nury T, Zarrouk A, Yammine A, Mackrill JJ, Vejux A, Lizard G. Oxiapoptophagy: A type of cell death induced by some oxysterols. Br J Pharmacol. 2021; 178(16):3115-23.

[49] Wright HL, McCarthy HS, Middleton J, Marshall MJ. RANK, RANKL and osteoprotegerin in bone biology and disease. Curr Rev Musculoskelet Med. 2009;2(1):56-64.

[50] Nakagawa N, Kinosaki M, Yamaguchi K, Shima N, Yasuda H, Yano K, et al. RANK is the essential signaling receptor for osteoclast differentiation factor in osteoclastogenesis. Biochem Biophys Res Commun. 1998;253(2):395-400

[51] Teitelbaum SL. Bone resorption by osteoclasts. Science. 2000;289(5484):1504-8.

[52] Takayanagi H, Kim S, Koga T, Nishina H, Isshiki M, Yoshida H, et al. Induction and activation of the transcription factor NFATc1 (NFAT2) integrate RANKL signaling in terminal differentiation of osteoclasts. Dev Cell. 2002;3(6):889-901

[53] Long CL, Humphrey MB. Osteoimmunology: the expanding role of immunoreceptors in osteoclasts and bone remodeling. Bonekey Rep. 2012;1.

[54] Ha H, Kwak HB, Lee SW, Jin HM, Kim HM, Kim HH, et al. Reactive oxygen species mediate RANK signaling in osteoclasts. Exp Cell Res. 2004;301(2):119-27.

[55] Agidigbi TS, Kim C. Reactive Oxygen Species in Osteoclast Differentiation and Possible Pharmaceutical Targets of ROS-Mediated Osteoclast Diseases. Int J Mol Sci. 2019;20(14).

[56] Tao H, Ge G, Liang X, Zhang W, Sun H, Li M, et al. ROS signaling cascades: dual regulations for osteoclast and osteoblast. Acta Biochim Biophys Sin (Shanghai). 2020;52(10):1055-62.

[57] Dugas B, Charbonnier S, Baarine M, Ragot K, Delmas D, Menetrier F, et al. Effects of oxysterols on cell viability, inflammatory cytokines, VEGF, and reactive oxygen species production on human retinal cells: cytoprotective effects and

prevention of VEGF secretion by resveratrol. Eur J Nutr. 2010;49(7):435-46.

[58] Wozniak E, Broncel M, Bukowska B, Gorzelak-Pabis P. The Protective Effect of Dabigatran and Rivaroxaban on DNA Oxidative Changes in a Model of Vascular Endothelial Damage with Oxidized Cholesterol. Int J Mol Sci. 2020;21(6).

[59] Choi YK, Kim YS, Choi IY, Kim SW, Kim WK. 25-hydroxycholesterol induces mitochondria-dependent apoptosis via activation of glycogen synthase kinase-3beta in PC12 cells. Free Radic Res. 2008;42(6):544-53.

[60] Joffre C, Leclere L, Buteau B, Martine L, Cabaret S, Malvitte L, et al. Oxysterols induced inflammation and oxidation in primary porcine retinal pigment epithelial cells. Curr Eye Res. 2007;32(3):271-80.

[61] Wang Y, Lebowitz D, Sun C, Thang H, Grynpas MD, Glogauer M. Identifying the relative contributions of Rac1 and Rac2 to osteoclastogenesis. J Bone Miner Res. 2008;23(2):260-70.

[62] Ueyama T, Geiszt M, Leto TL. Involvement of Rac1 in activation of multicomponent Nox1- and Nox3-based NADPH oxidases. Mol Cell Biol. 2006;26(6):2160-74.

[63] Daugaard M, Nitsch R, Razaghi B, McDonald L, Jarrar A, Torrino S, et al. Hace1 controls ROS generation of vertebrate Rac1-dependent NADPH oxidase complexes. Nat Commun. 2013;4:2180.

[64] Kvietys PR, Granger DN. Role of reactive oxygen and nitrogen species in the vascular responses to inflammation. Free Radic Biol Med. 2012;52(3):556-92.

[65] Fujihara R, Usui M, Yamamoto G, Nishii K, Tsukamoto Y, Okamatsu Y, et al. Tumor necrosis factor-alpha enhances RANKL expression in gingival epithelial cells via protein kinase A signaling. J Periodontal Res. 2014;49(4):508-17.

[66] Wu L, Guo Q, Yang J, Ni B. Tumor Necrosis Factor Alpha Promotes Osteoclast Formation Via PI3K/Akt Pathway-Mediated Blimp1 Expression Upregulation. J Cell Biochem. 2017;118(6):1308-15.

[67] Zhang YH, Heulsmann A, Tondravi MM, Mukherjee A, Abu-Amer Y. Tumor necrosis factor-alpha (TNF) stimulates RANKL-induced osteoclastogenesis via coupling of TNF type 1 receptor and RANK signaling pathways. J Biol Chem. 2001;276(1): 563-8.

[68] Tamura T, Udagawa N, Takahashi N, Miyaura C, Tanaka S, Yamada Y, et al.

Soluble interleukin-6 receptor triggers osteoclast formation by interleukin 6. Proc Natl Acad Sci U S A. 1993;90(24):11924-8.

[69] Wu Q, Zhou X, Huang D, Ji Y, Kang F. IL-6 Enhances Osteocyte-Mediated Osteoclastogenesis by Promoting JAK2 and RANKL Activity In Vitro. Cell Physiol Biochem. 2017;41(4):1360-9.

[70] Kudo O, Sabokbar A, Pocock A, Itonaga I, Fujikawa Y, Athanasou NA. Interleukin-6 and interleukin-11 support human osteoclast formation by a RANKL-independent mechanism. Bone. 2003;32(1):1-7.

[71] Ahmed SM, Luo L, Namani A, Wang XJ, Tang X. Nrf2 signaling pathway: Pivotal roles in inflammation. Biochim Biophys Acta Mol Basis Dis. 2017;1863(2):585-97.

[72] Braun S, Hanselmann C, Gassmann MG, auf dem Keller U, Born-Berclaz C, Chan K, et al. Nrf2 transcription factor, a novel target of keratinocyte growth factor action which regulates gene expression and inflammation in the healing skin wound. Mol Cell Biol. 2002;22(15):5492-505.

[73] Chen XL, Dodd G, Thomas S, Zhang X, Wasserman MA, Rovin BH, et al. Activation of Nrf2/ARE pathway protects endothelial cells from oxidant injury and inhibits inflammatory gene expression. Am J Physiol Heart Circ Physiol. 2006; 290(5):H1862-70.

[74] Kanzaki H, Shinohara F, Itohiya K, Yamaguchi Y, Katsumata Y, Matsuzawa M, et al. RANKL induces Bach1 nuclear import and attenuates Nrf2-mediated antioxidant enzymes, thereby augmenting intracellular reactive oxygen species signaling and osteoclastogenesis in mice. FASEB J. 2017;31(2):781-92.

[75] Sun X, Xie Z, Hu B, Zhang B, Ma Y, Pan X, et al. The Nrf2 activator RTA-408 attenuates osteoclastogenesis by inhibiting STING dependent NF-kappab signaling. Redox Biol. 2020;28:101309.

[76] Li W, Sun Y. Nrf2 is required for suppressing osteoclast RANKL-induced differentiation in RAW 264.7 cells via inactivating cannabinoid receptor type 2 with AM630. Regen Ther. 2020;14:191-5.

[77] Vijayan V, Wagener F, Immenschuh S. The macrophage heme-heme oxygenase-1 system and its role in inflammation. Biochem Pharmacol. 2018;153:159-67

[78] Bak SU, Kim S, Hwang HJ, Yun JA, Kim WS, Won MH, et al. Heme

oxygenase-1 (HO-1)/carbon monoxide (CO) axis suppresses RANKL-induced osteoclastic differentiation by inhibiting redox-sensitive NF-kappaB activation. BMB Rep. 2017;50(2):103-8.

[79] Huang H, Ryu J, Ha J, Chang EJ, Kim HJ, Kim HM, et al. Osteoclast differentiation requires TAK1 and MKK6 for NFATc1 induction and NF-kappaB transactivation by RANKL. Cell Death Differ. 2006;13(11):1879-91.

[80] Li Z, Chen C, Zhu X, Li Y, Yu R, Xu W. Glycyrrhizin Suppresses RANKL-Induced Osteoclastogenesis and Oxidative Stress Through Inhibiting NF-kappaB and MAPK and Activating AMPK/Nrf2. Calcif Tissue Int. 2018; 103(3):324-37.

TABLES

Table 1. Western blot antibody condition used in this study

W : Western blot C : Immunocytochemistry	Antibody	Company	Catalog No.	Dilution conditions	2nd antibody	Size (kDa)
	β-actin	Santa Cruz	sc-47778	1:5000	mouse	45
	Cathepsin K	Santa Cruz	sc-48353	1:1000	mouse	39
	c-fos	Santa Cruz	sc-8047	1:1000	mouse	62
	CH25H	Santa Cruz	sc-293256	1:2500	mouse	36
	COX-2	Cell signaling	12282	1:1000	rabbit	74
	HO-1	Santa Cruz	sc-3960991	1:1000	mouse	32
	iNOS	Abcam	ab15323	1:1000	rabbit	130
	IL-6	Santa Cruz	sc-57315	1:1000	mouse	21
	Lamin B1	Santa Cruz	sc-374015	1:2500	mouse	67
	NFATc1	Santa Cruz	sc-7294	1:500	mouse	90, 110 and 140
	NF-κB	Cell signaling	8242	1:1000(W)/1:250(C)	rabbit	65
	NOXO1	Santa Cruz	sc-390927	1:1000	mouse	27 and 39
	Nrf2	santa Cruz	sc-365949	1:1000	mouse	61
	MMP-2	Santa Cruz	sc-13595	1:1000	mouse	63
	MMP-9	Santa Cruz	sc-13520	1:1000	mouse	92
	OPG	Santa Cruz	sc-390518	1:1000	mouse	60
	phospho-NF-κB	Cell signaling	3036	1:1000	mouse	65
	Rac1/2/3	Santa Cruz	sc-514583	1:1000	mouse	22
	RANK	Santa Cruz	sc-374360	1:1000	mouse	66
	RANKL	Santa Cruz	sc-377079	1:1000	mouse	25, 35 and 40
	TRAF6	Santa Cruz	sc-8409	1:1000	mouse	60
	TNF-α	Santa Cruz	sc-52746	1:1000	mouse	26

Table 2. PCR primer sequences used in this study

PCR	Gene	Primer sequences	NCBI gene no.
	ch25h	Forward : 5'-CCATCTTCCCAGTCACCTTT-3' Reverse : 5'-GCTCCCAGAAGCTCATGTATT-3'	NM_009890.1
	gapdh	Forward : 5'-GGGTGTGAACCACGAGAAATA -3' Reverse : 5'-GTTGAAGTCGCAGGAGACAA-3'	NM_001289726.1

FIGURES

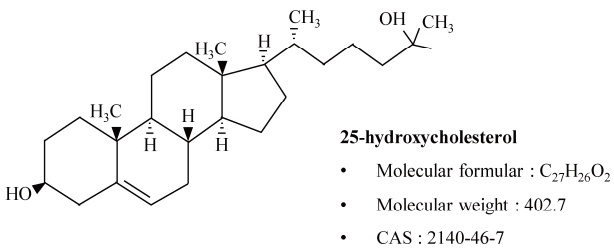

Figure 1. The chemical structure of 25-HC.

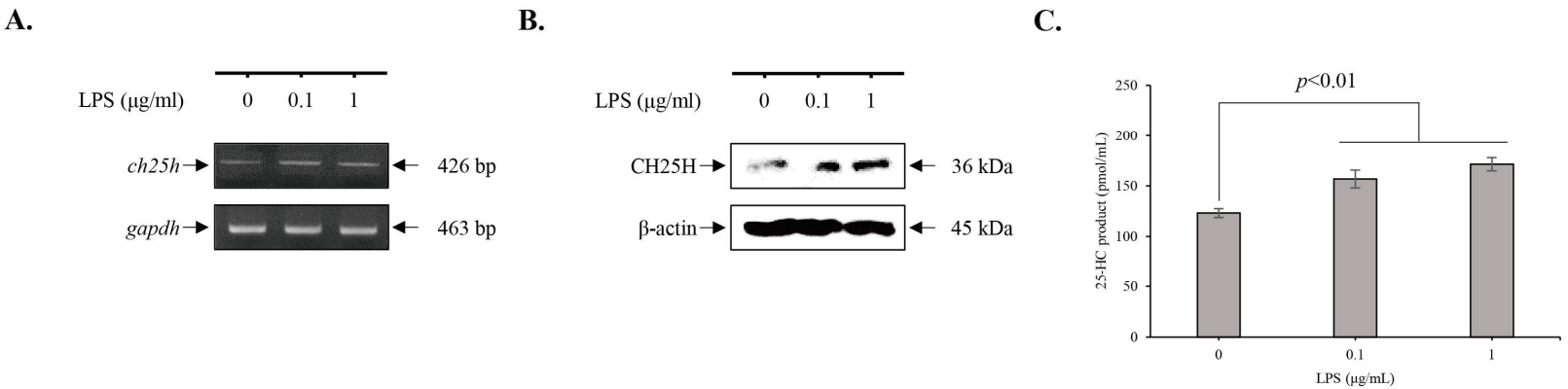

Figure 2. LPS upregulates the levels of CH25H and 25-HC in MDPC-23 cells. MDPC-23 cells were treated with 0 – 1 μg/mL LPS for 6 days. Total RNA and total proteins were extracted using TRIzol and cell lysis buffer, respectively. cDNA was synthesized from the extracted RNA and subjected to qPCR (A). Total proteins were subjected to SDS-PAGE using a 12% gel and western blotting using the anti-CH25H antibodies (B). GAPDH and β-actin were used as internal controls for qPCR and western blotting analyses, respectively. Conditioned media were collected from the MDPC-23 cells treated with LPS for 6 days and subjected to 25-HC ELISA, which was performed according to the manufacturer's instructions (C). A, The expression of CH25H, which encodes an enzyme that catalyzes the formation of 25-HC from cholesterol, was upregulated in the LPS-treated MDPC-23 cells. B, The expression of CH25H was upregulated in the LPS-induced MDPC-23 cells. C, The production of 25-HC was upregulated in the LPS-treated MDPC-23 cells.

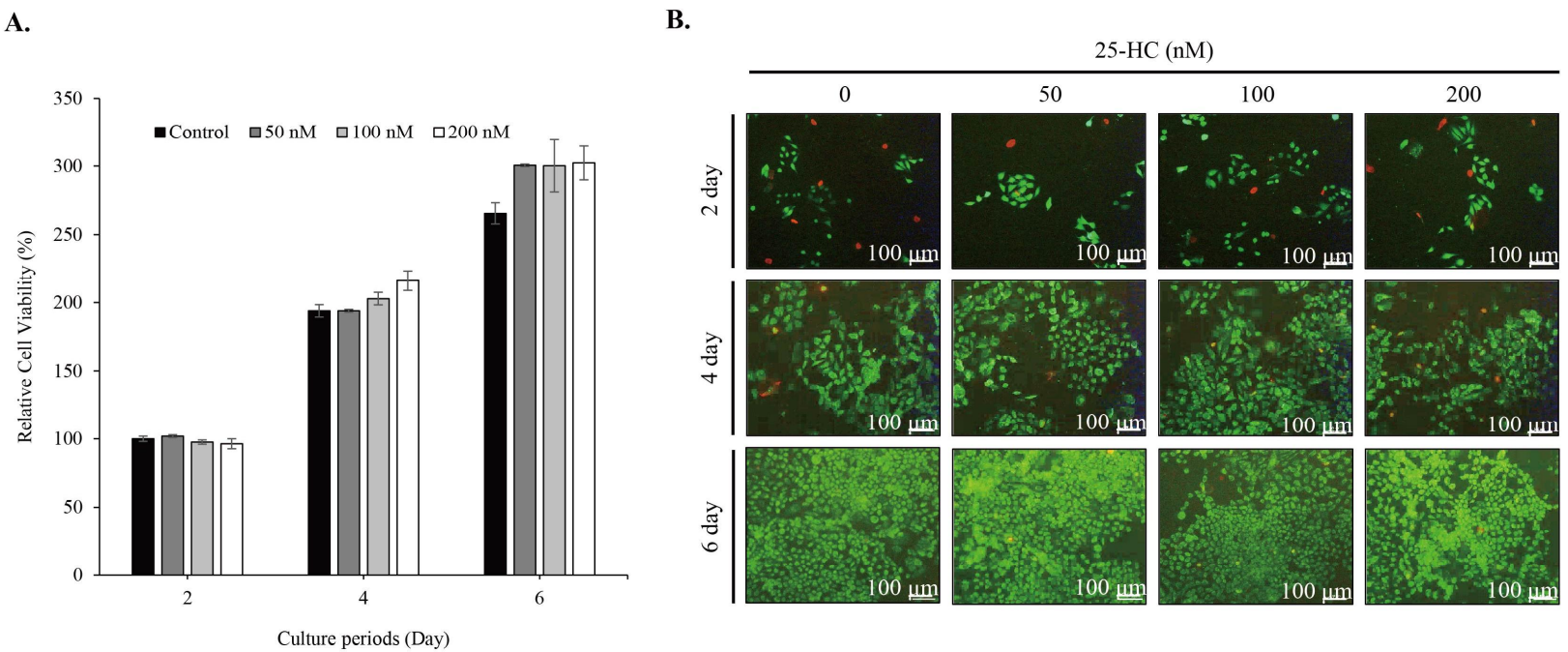

Figure 3. 25-HC does not affect the viability of MDPC-23 cells. MDPC-23 cells were treated with 50 – 200 nM of 25-HC for 2, 4, and 6 days. Cell viability assay was performed using cell counting kit-8 (CCK-8) (A), while the viability staining was performed using ethidium homodimer-1 (stains dead cells; red fluorescence) and green calcein AM (stains live cells; green fluorescence) (B). 25-HC did not affect A, the viability or B, the survival of MDPC-23 cells.

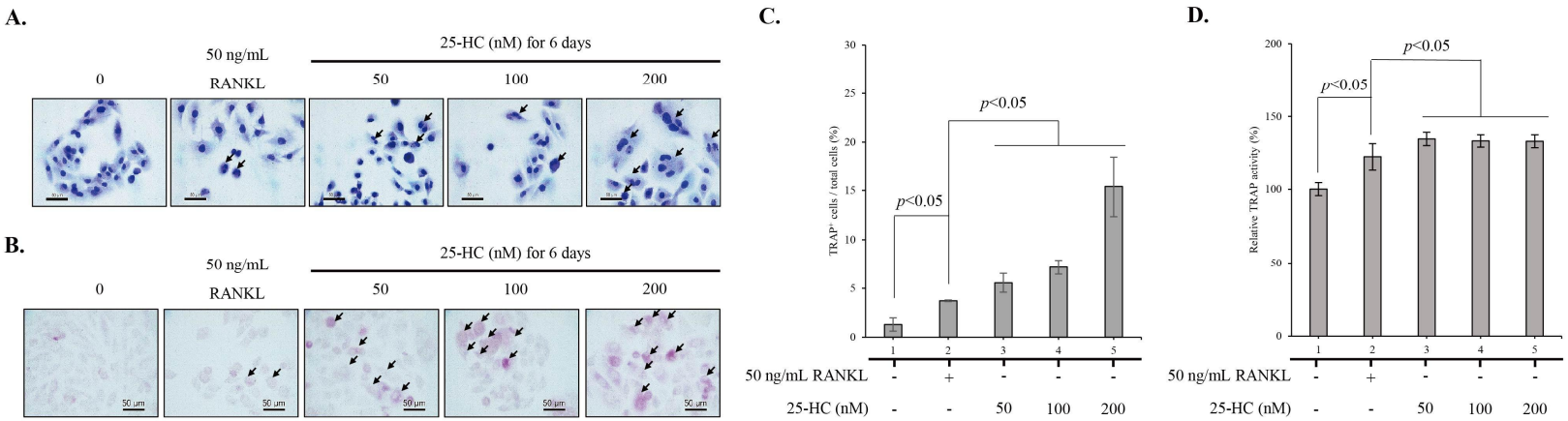

Figure 4. 25-HC increases the number of odontoclasts differentiated from MDPC-23 cells. MDPC-23 cells cultured in 8-well chamber slide were treated with 50 ng/mL RANKL or 50 – 200 nM of 25-HC for 6 days. The morphology of multinucleated cells and TRAP-positive odontoclast was investigated using H&E staining (A) and TRAP staining (B), respectively. The number of TRAP-positive cells was counted and presented as a histogram (C). TRAP activity assay (D) was performed, following the manufacturer's instructions. A, The number of multinucleated MDPC-23 cells in the 25-HC-treated group was higher than that in the RANKL (positive control)-treated group. B&C, The number of TRAP-positive odontoclasts differentiated from MDPC-23 in the 25-HC-treated group was higher than that in the RANKL. D, The activity of TRAP in the 25-HC-treated MDPC-23 cells was higher than that in the RANKL-treated MDPC-23 cells. Black arrows indicate odontoclasts that differentiated from MDPC-23 cells.

A.

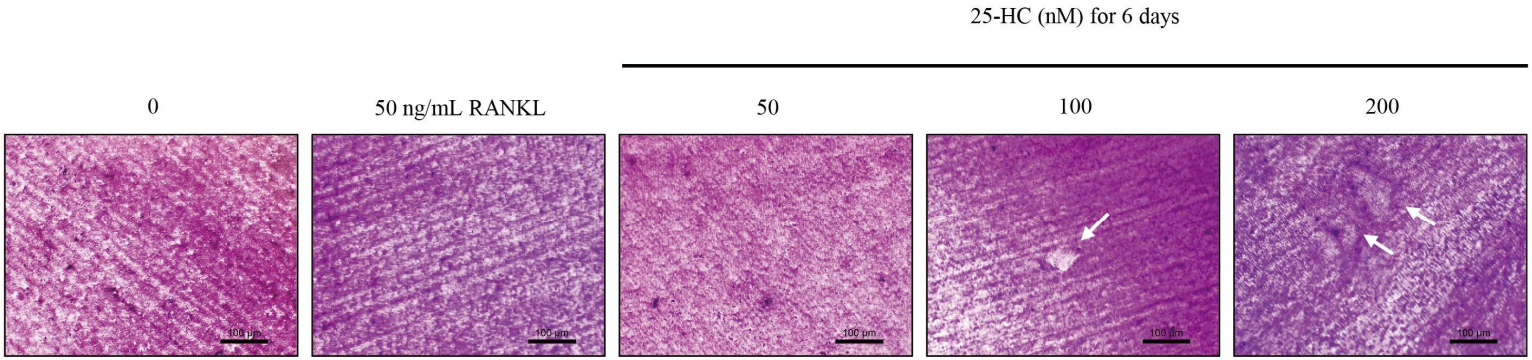

Figure 5. 25-HC promotes dentin resorption in the odontoclasts differentiated from MDPC-23 cells. MDPC-23 cells cultured on the dentin disc were treated with 50 ng/mL RANKL and 50 – 200 nM of 25-HC for 6 days. The dentin discs were rinsed with NaOCl and stained with toluidine blue O in 0.5% sodium tetraborate. The resorption pits were observed using a Leica DM750 microscope. White arrows indicate resorption pits on the dentin disc. Treatment with 25-HC promoted dentin resorption in odontoclasts differentiated from 25-HC-treated MDPC-23 cells. Additionally, the number of resorption pits in the 25-HC-treated group was higher than that in the RANKL-treated group

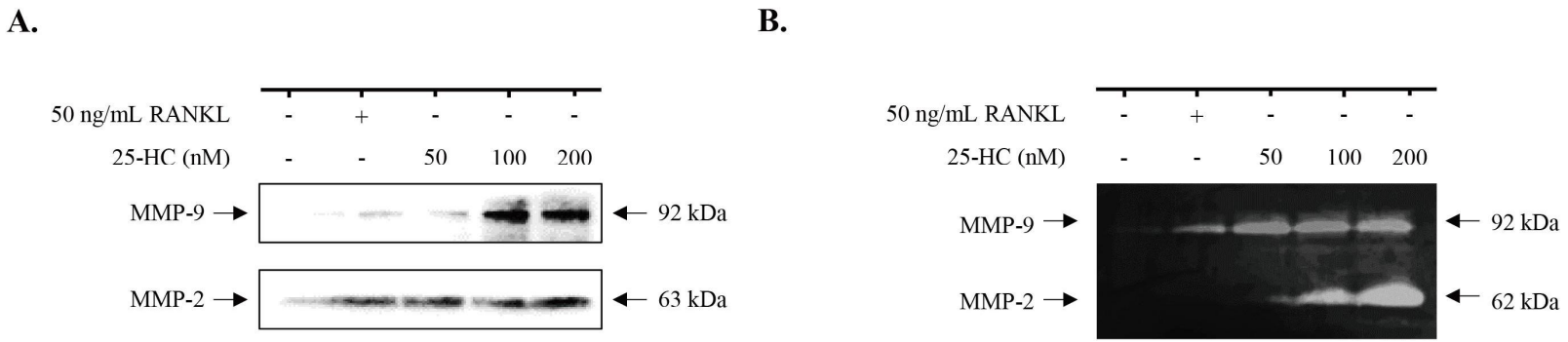

Figure 6. 25-HC promotes dentin resorption in odontoclasts differentiated from MDPC-23 cells through the upregulation and activation of MMPs. MDPC-23 cells were treated with 50 ng/mL RANKL or 50 – 200 nM of 25-HC for 6 days. Conditioned media were subjected to SDS-PAGE using a 12% gel and western blotting (A) using the anti-MMP-2 and MMP-9 antibodies. To verify the activation of MMPs such as MMP-2 and MMP-9, conditioned media were subjected to gelatin zymography (B). A, The expression levels of MMP-2 and MMP-9 were upregulated in the odontoclast differentiated from 25-HC-treated MDPC-23 cells. B, Treatment with 25-HC dose-dependently promoted the activity of MMPs.

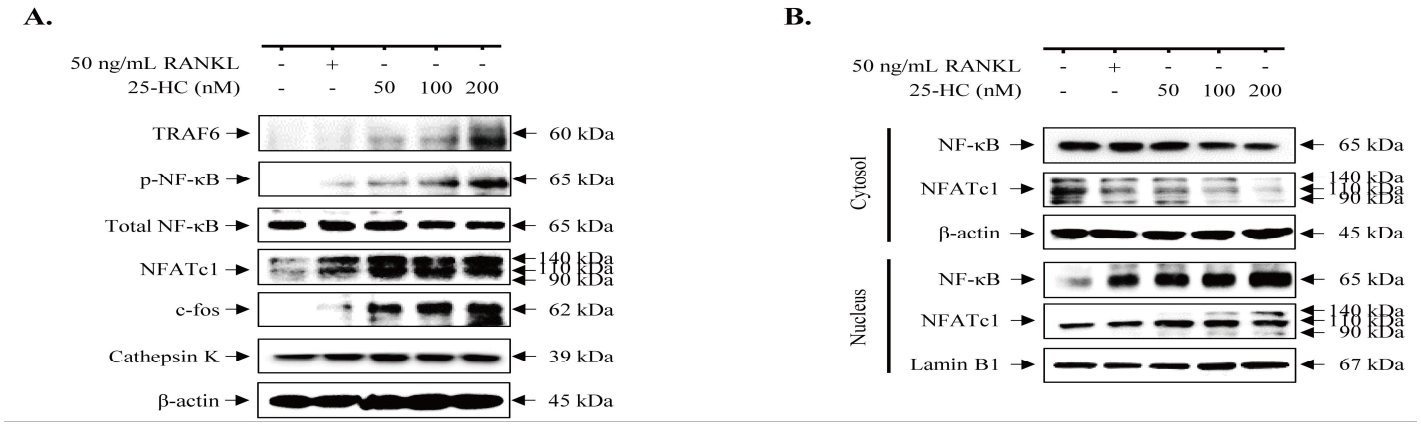

Figure 7. 25-HC promotes the expression of odontoclastogenic biomarkers and the nuclear translocation of NF-κB in MDPC-23 cells. MDPC-23 cells were treated with 50 ng/mL RANKL or 50 – 100 nM of 25-HC for 6 days. Total proteins were extracted from the cells and subjected to western blotting to detect odontoclastogenic specific markers, such as TRAF6, phospho-NF-κB, total NF-κB, NFATc1, c-fos, and cathepsin K. To verify the nuclear translocation of NF-κB from the cytosol, the nuclear and cytosolic proteins were extracted from the MDPC-23 cells treated with 50 ng/mL RANKL or 50 – 200 nM of 25-HC for 6 days and subjected to western blotting using the anti-NF-κB and anti-NFATc1 antibodies. β-actin and Lamin B1 were used for the normalization of cytosolic and nuclear proteins, respectively. A, Treatment with 25-HC upregulated the expression of odontoclastogenic biomarkers in MDPC-23 cells. B, NF-κB and its downstream transcription factor NFATc1 translocated from the cytosol to the nucleus in 25-HC-treated MDPC-23 cells.

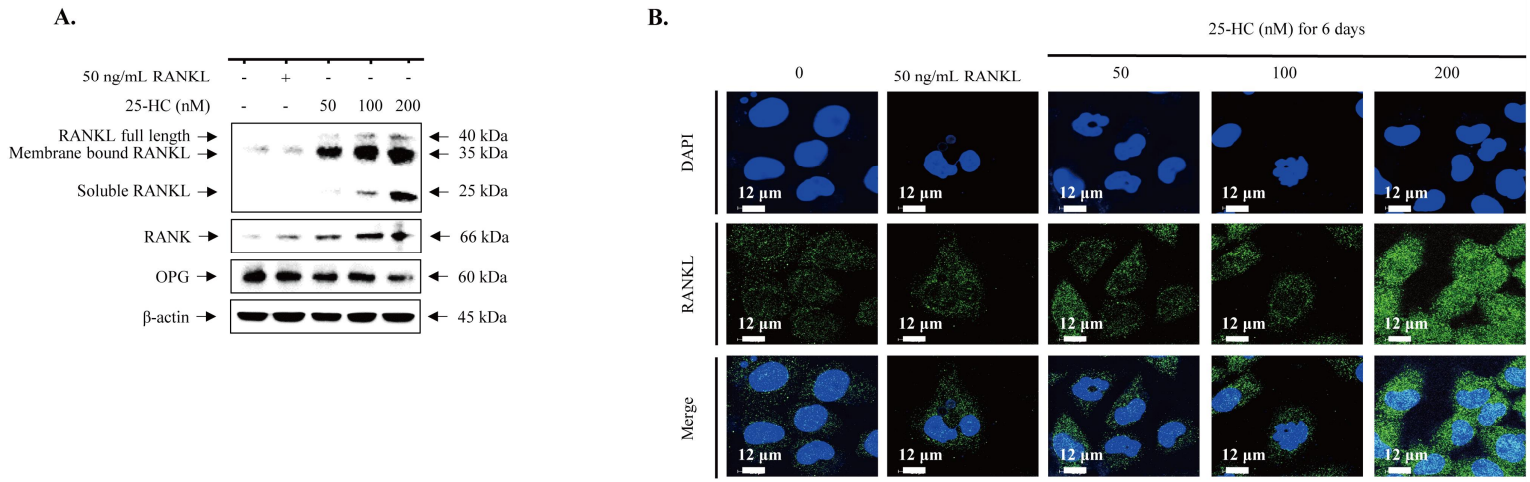

Figure 8. 25-HC promotes odontoclastogenesis in MDPC-23 cells through the upregulation of RANKL and RANK and the downregulation of OPG. MDPC-23 cells were treated with 50 ng/mL RANKL or 50 – 200 nM of 25-HC for 6 days. Total proteins were extracted from the cells and subjected to western blotting (A) using the anti-RANKL, anti-RANK, and anti-OPG specific antibodies. β-actin was used as an internal control. To confirm the expression of RANKL in 25-HC-treated MDPC-23 cells, cells cultured in an 8-well chamber slide were treated with 50 ng/mL RANKL or 50 – 200 nM of 25-HC for 6 days. The cells were then fixed with 4% paraformaldehyde and incubated with the anti-RANKL-specific antibodies for 12 h at 4°C. Next, the cells were incubated with DAPI and Alexa 488-conjugated secondary antibodies for 1 h. Finally, images were captured using a laser confocal scanning microscope system (B). A, 25-HC-induced odontoclastogenesis was mediated by the upregulation of RANKL and RANK and the downregulation of OPG in MDPC-23 cells. B, RANKL was significantly upregulated in 25-HC-treated MDPC-23 cells.

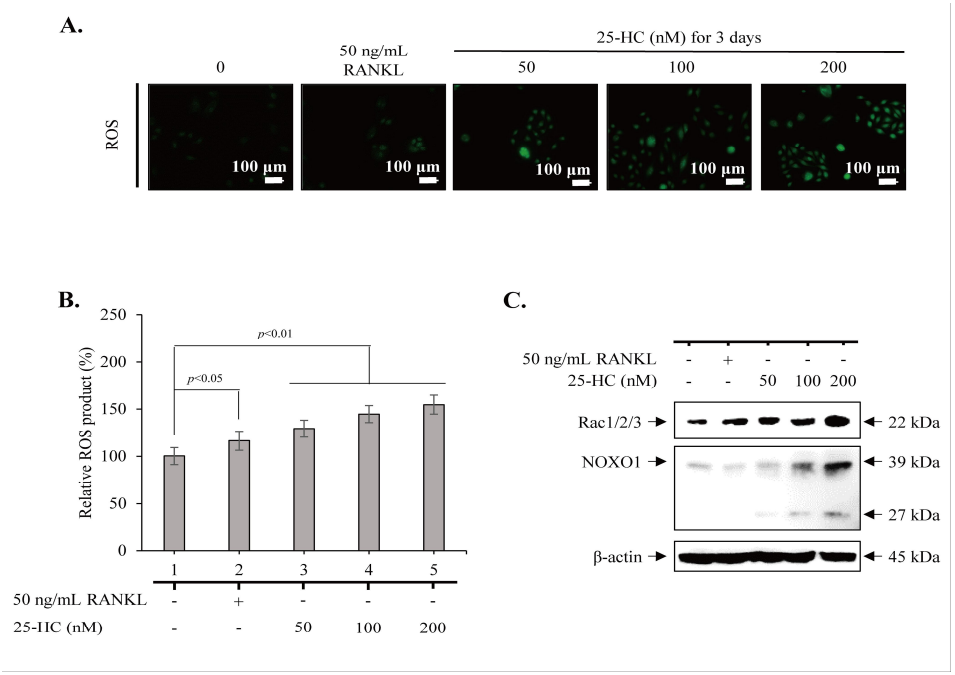

Figure 9. 25-HC promotes ROS production in MDPC-23 cells through the Rac1/2/3-NOXO1 axis. MDPC-23 cells were treated with 50 ng/mL RANKL or 50 – 200 nM of 25-HC for 3 days. The production of ROS was determined using H2DCF-DA staining (A) and ROS production assay (B). Total proteins were extracted from the cells and subjected to western blotting using the anti-Rac1/2/3 and NOXO1 antibodies (C). A&B, The production of ROS was upregulated in 25-HC-treated MDPC-23 cells. C, In MDPC-23 cells, 25-HC-induced ROS production was mediated by the Rac1/2/3-NOXO1 axis in MDPC-23 cells.

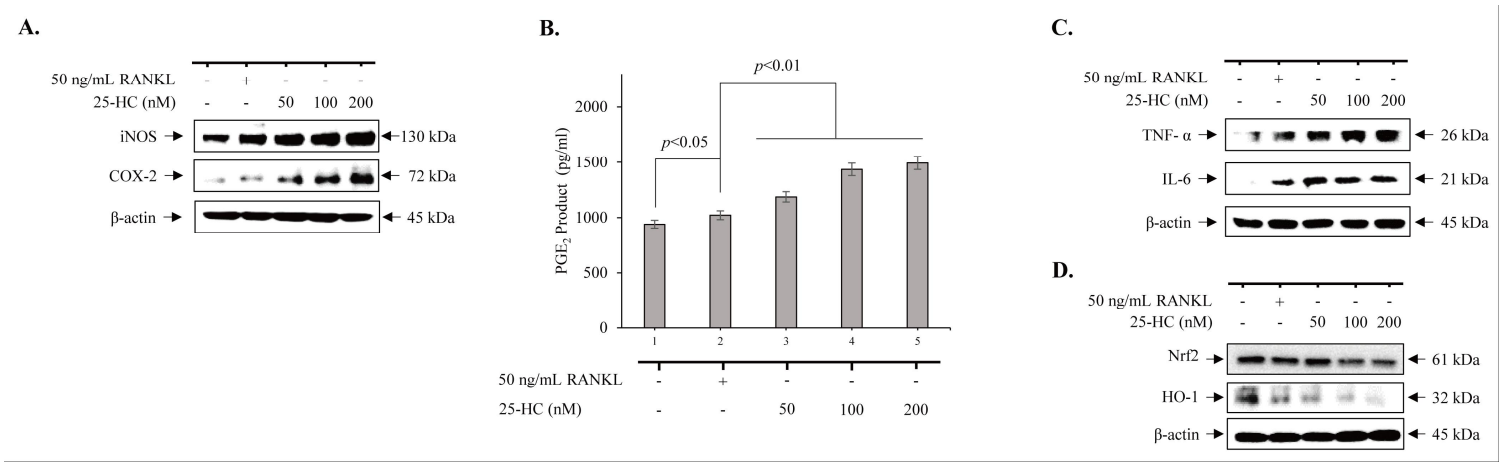

Figure 10. 25-HC upregulates the expression of inflammatory mediators and pro-inflammatory cytokines in MDPC-23 cells through the modulation of Nrf2-HO-1 axis. MDPC-23 cells were treated with 50 ng/mL RANKL or 50 – 200 nM of 25-HC for 6 days. Total proteins were extracted from the cells and subjected to western blotting using the anti-iNOS, anti-COX-2, anti-TNF-α, anti-IL-6, anti-Nrf2, and anti-HO-1. Additionally, PGE_2 assay was performed to examine the production of PGE_2 in MDPC-23 cells treated with 50 ng/mL RANKL or 50 – 200 nM of 25-HC for 6 days. A, The expression levels of inflammatory mediators, such as iNOS and COX-2 were significantly upregulated in 25-HC-treated MDPC-23 cells. B, The production of the inflammatory mediator PGE_2 was significantly upregulated in 25-HC-treated MDPC-23 cells. C, The levels of pro-inflammatory cytokines, such as TNF-α and IL-6 were significantly upregulated in 25-HC-treated MDPC-23 cells. D, The expression levels of Nrf2 and HO-1 were downregulated in 25-HC-treated MDPC-23 cells.

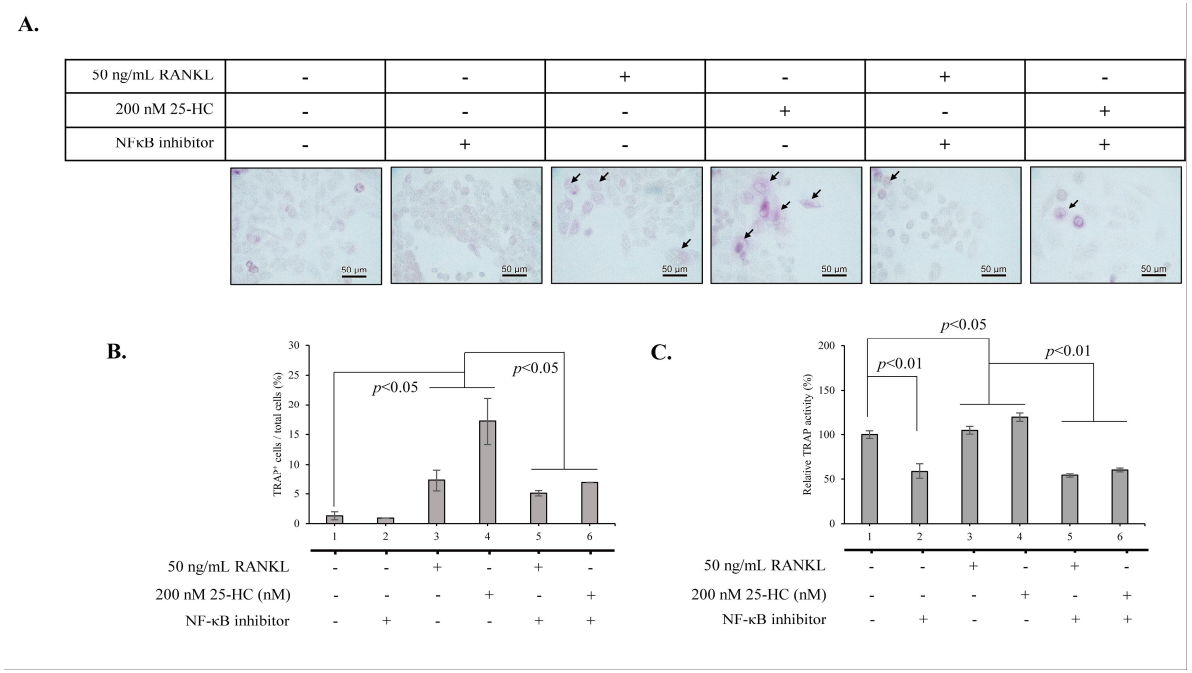

Figure 11. NF-κB inhibitor suppresses odontoclastogenesis in 25-HC-treated MDPC-23 cells. MDPC-23 cells were treated with 50 ng/mL RANKL or 50 – 100 nM of 25-HC in the presence or absence of the CDDO-Me for 6 days. TRAP staining was performed to stain the odontoclast. A, CDDO-Me mitigated the 25-HC-induced formation of odontoclasts in MDPC-23 cells. B, Treatment with CDDO-Me decreased the number of TRAP positive odontoclasts in 25-HC-treated MDPC-23 cells. C, Treatment with CDDO-Me decreased the activity of TRAP in 25-HC-treated MDPC-23 cells.

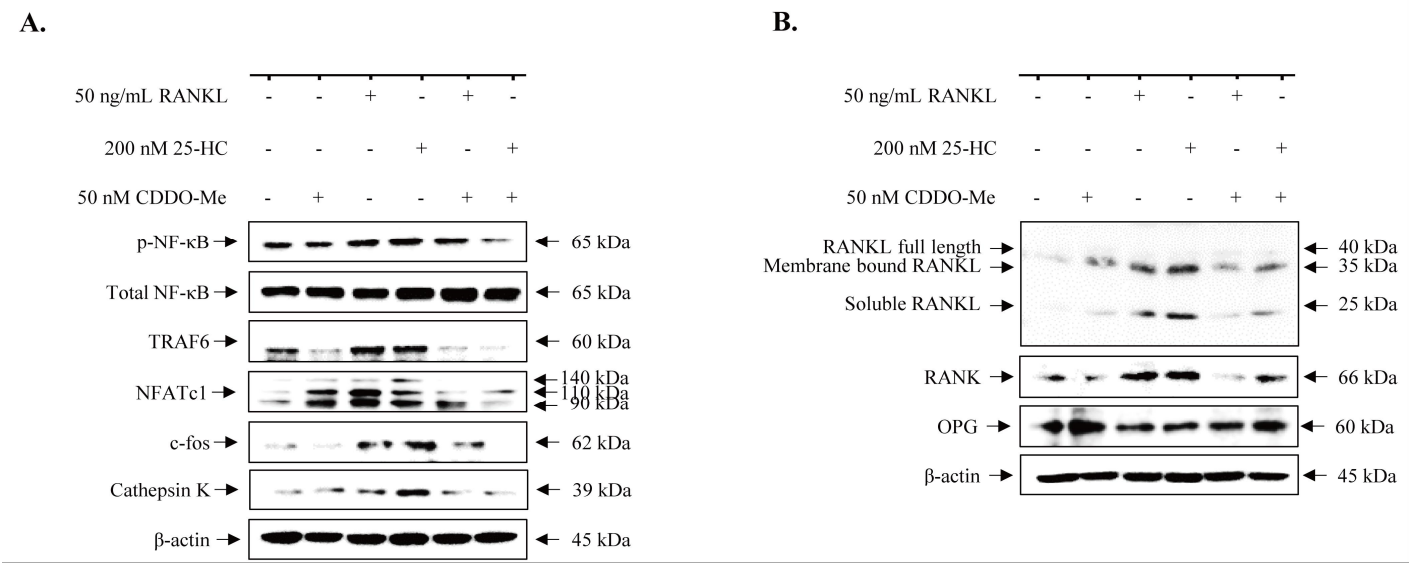

Figure 12. NF-κB inhibitor suppresses the expression of odontoclastogenic factors in 25-HC-treated MDPC-23 cells. MDPC-23 cells were treated with 50 ng/mL RANKL or 50 – 100 nM of 25-HC in the presence or absence of the CDDO-Me for 6 days. Total proteins were extracted and the expression levels of odontoclastogenic factors, such as TRAF6, phospho-NF-κB, total NF-κB, NFATc1, c-fos, cathepsin K, RANKL, and RANK were examined. A, CDDO-Me mitigated the 25-HC-induced upregulation of TRAF6, phospho-NF-κB, total NF-κB, NFATc1, c-fos and cathepsin K in MDPC-23 cells. B, CDDO-Me downregulated the expression of RANKL and RANK and upregulated the expression of OPG in 25-HC-treated MDPC-23 cells.

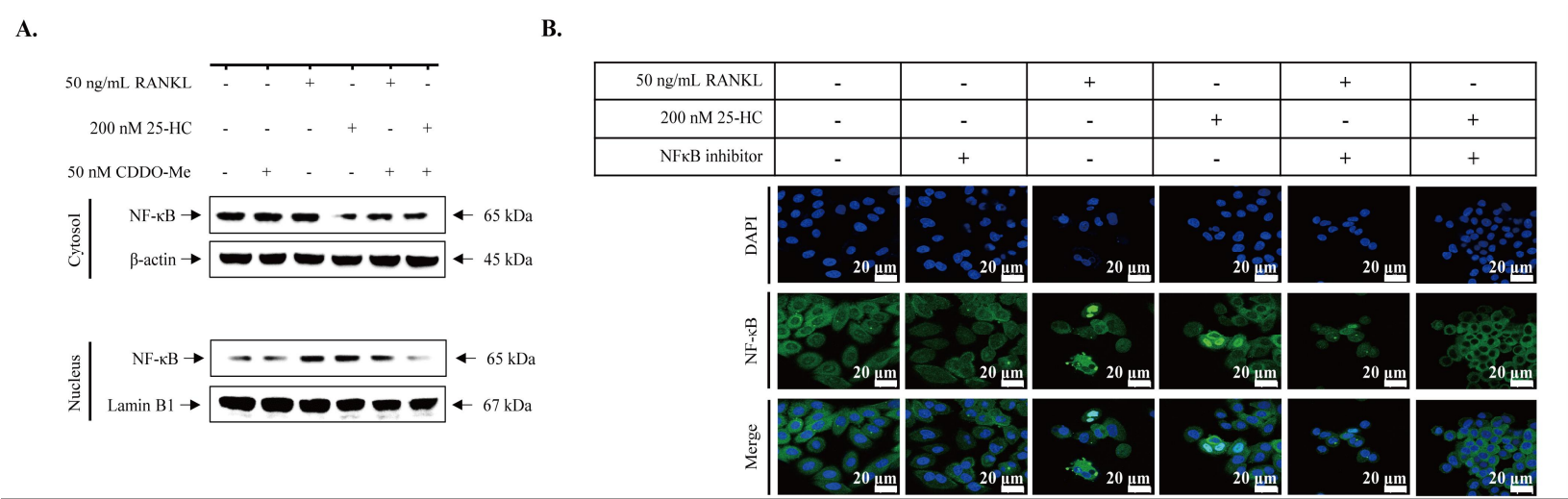

Figure 13. 25-HC induces odontoclastogenesis through the modulation of the NF-κB signaling pathway in MDPC-23 cells. MDPC-23 cells were treated with 50 ng/mL RANKL or 200 nM of 25-HC in the presence or absence of the CDDO-Me for 6 days. The nuclear and cytosolic proteins were extracted and subjected to western blotting analysis using the anti-NF-κB antibodies (A). After culturing under identical culture conditions, the cells were fixed using 4% paraformaldehyde and incubated with the anti-NF-κB specific antibodies for 12 h at 4℃. Next, the cells were incubated with DAPI and Alexa 488-conjugated secondary antibodies for 1 h. Finally, images were captured using a laser confocal scanning microscope system (B). A, Treatment with CDDO-Me significantly mitigated the 25-HC-induced nuclear translocation of NF-κB. B, CDDO-Me mitigated 25-HC-induced NF-κB nuclear translocation in the MDPC-23 cells.

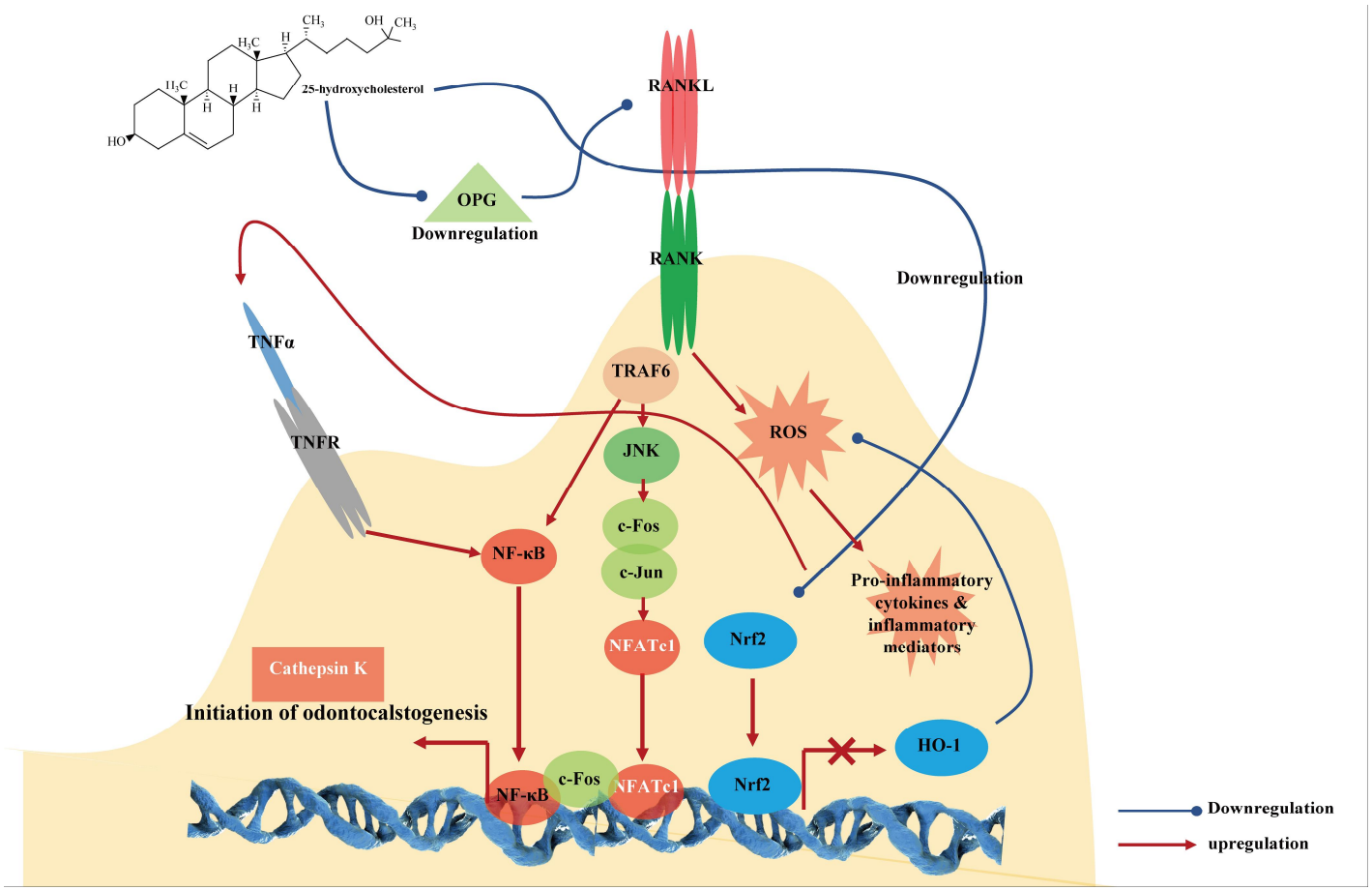

Figure 14. The schematic diagram of 25-HC-induced odontoclastogenesis in the MDCP-23 cells.

국 문 초 록

MDPC-23 상아질모세포에서 25-Hydroxycholesterol에 의한 파치세포화

임 향 이
조선대학교 대학원 치의생명공학과
(지도교수 :김 재 성)

콜레스테롤로부터 합성되는 옥시스테롤 중의 하나인 25-hydroxycholesterol(25-HC)은 염증을 매개로하여 cholesterol 25-hydroxylase(CH25H)에 의해 합성된다. 본 연구에서는 MDPC-23 상아질모세포에서 25-HC에 의한 파치세포 분화유도와 그 신호전달기전을 분석하였다.

본 연구의 목적을 위해, MDPC-23 상아질모세포에서 25-HC을 이용하여 파치세포로 분화를 유도한 후, CCK-8 분석, 세포 live&dead 분석, hematoxylin & eosin 분석, TRAP 활성 및 발현 분석, 상아질 재흡수 분석, gelatin zymography 분석, western blot 분석, ROS 생성 분석, prostaglandin E_2(PGE_2) 생성 분석, immunocytochemistry 분석 등을 시행하였다.

25-HC은 MDPC-23 상아질모세포에서 tartrate-resistant acid phosphatase(TRAP) 활성을 농도 의존적으로 증가시켰다. 25-HC에 의해 분화된 상아질모세포에서 파치세포의 특징 중 하나인 다핵구의 형성과 matrix metalloproteinase(MMP)-9, -2의 발현과 활성이 증가함을 관찰할 수 있었으며, 이러한 결과는 25-HC에 의한 상아질모세포의 파치세포 분화유도를 나타낸다. 또한 25-HC은 RANKL의 발현을 농도 의존적으로 증가시켰으며, 이와 관련된 염증인자인 iNOS, COX-2, PGE_2, TNF-α 및 IL-6의 단백질 발현을 증가시켰다. 25-HC은 상아질모세포에서 파치세포 분화의 신호전달기전 바이오마커인 TRAF6, nuclear factor-κB(NF-κB), NFATc1, c-fos 및 cathepsin K의 발현을 증가시켰으며, NFATc1과 NF-κB의 핵으로의 이동 역시 증가시켰다. 뿐만 아니라 NF-κB 신호전달 억제 시 25-HC에 의한 상아질모세포의 파치세포 분화유

도 또한 억제되었다.

본 연구의 결과는 25-HC가 MDPC-23 상아질모세포의 염증을 유도할 뿐만 아니라, 파치세포로의 분화를 유도할 수 있음을 시사한다. 또한 본 연구의 결과는 옥시스테롤 25-HC가 상아질 내흡수와 관련되어 있으며, 상아질 내흡수의 새로운 병인 중 하나로 작용할 수 있음을 시사한다.